What processes drive the ocean heat transport?

What processes drive the ocean heat transport?

RAFFAELE FERRARI AND DAVID FERREIRA

Department of Earth, Atmospheric and Planetary Sciences,

Massachusetts Institute of Technology,

Cambridge USA.

Submitted, *Ocean Modelling,*

February 20, 2011

Corresponding author address:

EAPS, 77 Massachusetts Avenue, Cambridge, MA, 02139, USA. Email: rferrari@mit.edu.

ABSTRACT

The ocean contributes to regulating the Earth's climate through its ability to transport heat from the equator to the poles. In this study we use long simulations of an ocean model to investigate whether the heat transport is carried primarily by wind-driven gyres or whether it is dominated by deep circulations associated with abyssal mixing and high latitude convection. The heat transport is computed as a function of temperature classes. In the Pacific and Indian ocean, the bulk of the heat transport is associated with wind-driven gyres confined to the thermocline. In the Atlantic, the thermocline gyres account for only 40% of the total heat transport. The remaining 60% is associated with a circulation reaching down to cold waters below the thermocline. Using a series of sensitivity experiments, we show that this deep heat transport is primarily set by the strength and patterns of surface winds and only secondarily by diabatic processes at high latitudes in the North Atlantic. Abyssal mixing below 2,000m has hardly any impact on ocean heat transport. A major implication is that the role of the ocean in regulating Earth's climate strongly depends on how surface winds change across different climates in both hemispheres at low and high latitudes.

1. Introduction

One of the most important contributions the ocean makes to the Earth's climate is through its poleward heat transport. The ocean transports 3 PW of heat out of the tropics or more than 50% of that accomplished by the ocean-atmosphere system, while its contribution at higher latitudes is less than 10% of the total. This heat is transported by a combination of shallow wind-driven gyres confined to the tropics and subtropics, and deep circulations connected to high-latitude convection. The partitioning of the ocean heat transport (OHT) among these different circulations has important implications for our understanding of the climate system. The OHT associated with different circulations is affected by different physical processes and identifying which circulations dominate the OHT is tantamount to determining what oceanic processes control the OHT and more generally the climate. For instance, if abyssal circulations were responsible for much of the OHT, then climate would be sensitive to the strength of abyssal mixing (e.g. Simmons et al. 2004). If, on the other hand, North Atlantic Deep Water (NADW) formation were critical, then high latitude air-sea fluxes would be a crucial element of the climate system (e.g. Rahmstorf 2002). Finally, if the shallow circulations of the tropics and subtropics were responsible for transporting most of the heat, then winds alone would be key in regulating climate (e.g. Held 2001).

The goal of this study is to quantify the pathways of ocean heat transport and the processes that drive it. Note that this work differs from the vast literature on the meridional mass transport (see references in Wunsch and Ferrari 2004). The OHT depends both on the surface winds, that drive the mass transport, and on the air-sea fluxes, that set the temperature distribution. Hence changes in OHT across different climates cannot be explained uniquely in terms of changes in the ocean overturning circulation.

Despite its centrality to our understanding of the climate system, the vertical structure of the OHT is poorly known. Hall and Bryden (1982) and Roemmich and Wunsch (1985) analyzed hydrographic measurements and concluded that in the North Atlantic the OHT is achieved through the meridional overturning circulation associated with deep flows, while in the North Pacific the

OHT is accomplished by the horizontal gyroscopic circulation forced by surface winds. This conclusion was based on integral measures that separated the OHT between vertical and horizontal circulations–the former was interpreted as due to deep circulations and the latter as due to wind-driven circulations. However, this separation does not take into account the fact that *all* circulations have both a vertical and a horizontal component, so that a true distinction is not possible in this framework.

More recently Talley (2003) has attempted to estimate the vertical structure of the OHT by separating the transport associated with shallow, intermediate, and deep waters. She concluded that, in the North Atlantic, the deep overturning contributes only 60% of the OHT, a fraction much smaller than previously estimated. However her results depends on a number of assumptions on the pathways of different circulations. A clear way of diagnosing the vertical structure of the OHT is still lacking.

Boccaletti et al. (2005) introduced the concept of *heatfunction* to quantify the structure of the OHT. The heatfunction is a two-dimensional representation of the three dimensional pathways of heat in the ocean. It allows to separate the contribution that shallow and deep circulations make to the total OHT. Boccaletti and collaborators used the heatfunction to study the partitioning of the OHT in a numerical model of the global ocean. Greatbatch and Zhai (2007) extended the definition and applied it to climatological data. In both studies the heatfunction indicates that most pathways of heat in the ocean are surface intensified and confined to tropical and subtropical latitudes. These results strongly suggest that the OHT is primarily sensitive to low-latitude winds and less to abyssal mixing and high latitude air-sea fluxes. However a detailed quantitative study of how different oceanic processes affect OHT is still lacking.

The main goal of this paper is to complete the analysis in Boccaletti et al. (2005) and estimate the relative importance of winds, abyssal mixing, and surface fluxes in setting the strength and patterns of OHT. This is done by first extending the definition of heatfunction by working in temperature coordinates. The new definition has a simpler interpretation and is easier to compute. Then the heatfunction is used to quantify how the OHT changes in a series of sensitivity

experiments in which we suppress convection with traditional water-hosing experiments, enhance abyssal mixing, and change surface winds.

The series of sensitivity experiments confirm that changes in high-latitude convection do interfere with NADW formation, modify the deep circulations and reduce the OHT associated with that circulation. Abyssal mixing, instead, has no effect on OHT transport, because it only affects cold abyssal circulations that do not transport significant OHT. Most importantly the sensitivity to surface winds dominates the response: both surface and deep circulations are modified by changes in the winds. Focusing on the North Atlantic, we show that cross-equatorial OHT, a feature which is often invoked as proof of the overwhelming role of the deep overturning (and therefore of high latitude convection) is in reality as sensitive to winds as the shallow circulation. This suggests that the OHT is very sensitive to changes in winds across different climates, probably even more than to changes in air-sea fluxes.

The structure of the paper is as follows. In section 2, we introduce the concept of heatfunction in temperature coordinates and we compare it to the definition used by Boccaletti et al. (2005) and Greatbatch and Zhai (2007). Section 3 introduces the numerical model used for this study. The climatology, heat transport and heatfuction for the control run are presented in section 4. The sensitivity of OHT to changes in mixing coefficients, high latitude buoyancy forcing, and winds are discussed in section 5. Finally, in section 6, we offer our conclusions.

2. Heatfunction

The goal of this paper is to quantify the meridional transport of heat by the various branches of the ocean circulation. The ocean heat content is given by the product of the specific heat capacity of seawater, c_p, and the potential temperature referenced to the surface, θ. McDougall (2003) gives a detailed discussion of how $c_p\theta$ with a constant c_p approximates the oceanic heat content. He also shows that a better approximation is obtained by replacing potential temperature with conservative temperature. Here we will present the analysis in terms of potential temperature, the

variable used in our numerical model. However the analysis could be easily carried through in terms of conservative temperature. Following common practice, we will use interchangeably the terms temperature and heat content, but the reader should be aware that heat content is the proper physical variable.

The overturning circulations of the global ocean are often represented in terms of the streamfunction associated with the zonally integrated velocity field. Boccaletti et al. (2005) have recently shown that the oceanic pathways of heat can be analogously represented in terms of a heatfunction associated with the zonally integrated heat fluxes. The definition is analogous to that of the streamfunction with one important difference. Only waters that change temperature along closed overturning circulations contribute a meridional OHT. Waters that flow poleward and return equatorward at the same temperature, in the zonal mean, do not contribute any net meridional heat exchange. Hence the heatfunction must be computed only from the heat flux that is associated with waters changing temperature along closed circulations. The idea is straightforward, but the actual calculation is technically challenging because of the numerous interpolation steps necessary to separate the different portions of the heat flux.

In this paper we adopt an approach similar to that of Boccaletti et al. (2005), but we take zonal integrals at fixed temperature instead of fixed depth. By averaging at fixed temperature, we automatically filter out any recirculation of waters at constant temperature. This avoids the problem of eliminating the part of the heat flux not associated with OHT. The advantages are not only conceptual, but also practical because the interpolation steps necessary to compute the heatfunction are dramatically reduced.

Notice that this paper focuses on heat transport and hence we sketch the derivation of the heat streamfunction, i.e. the heatfunction. However the derivation can be applied to any oceanic tracer like salt, chemical and organic tracers. All one needs to do is replace θ with the tracer of choice in the pages that follow. That means that one replaces the averaging along temperature surfaces with averaging along tracer isosurfaces. No restrictions apply: the tracer can have sources and sinks and its profiles do not have to be monotonously increasing or decreasing. The resulting tracer

streamfunction will describe the lines along which the tracer is transported in a zonally averaged sense.

The heatfunction formalism introduced here applies only for steady state problems, i.e. the tracer budget must be in steady state. In practice one can take a long time average of the tracer budget to minimize its variability. An extension of this work for transient tracer budgets is left for a future study.

a. Heatfunction in two dimensions

Heat is transported poleward by the ocean if, on average, waters moving polewards are compensated by an equatorward flow at colder temperature. It is useful to illustrate how the OHT is achieved in a two dimensional flow taken to represent the zonally averaged ocean circulation. The meridional OHT by a two dimensional circulation in the latitude-depth ($y - z$) plane is given by,

$$H = \rho_0 c_p \int v\theta \ \mathrm{d}z = \rho_0 c_p \int -\frac{\partial \psi}{\partial z}\theta \ \mathrm{d}z = \rho_0 c_p \int \frac{\partial \theta}{\partial z}\psi \ \mathrm{d}z = \rho_0 c_p \int \psi \ \mathrm{d}\theta, \tag{1}$$

where ρ_0 is a reference ocean density. In deriving the above we have written v=-$\partial\psi/\partial z$, in which ψ is the streamfunction for the volume transport, and we made use of the fact that ψ=0 at the top and bottom of the two dimensional ocean. We also assumed that temperature is a decreasing function of depth to convert the integral from z to θ-coordinates (this restriction is relaxed below). The relationship $H = \rho_0 c_p \int \psi \mathrm{d}\theta$ tells us that the OHT by oceanic flows can be expressed in terms of the mass transport in temperature layers. This is the basic concept behind the definition of the heatfunction. The next section describes how to extend the formalism to three dimensions.

Bryan and Sarmiento (1985), Klinger and Marotzke (2000), and Vallis and Farneti (2009) went through a very similar argument to show that the OHT is given by the integral of the mass streamfunction in temperature layers. Vallis and Farneti went a step forward and used this relationship to compute the heat transport associated with surface and deep overturning circulations by splitting the integral in two parts. The first integral was taken from the surface temperature to the temperature separating surface and deep circulations, while the second integral was taken

over the remaining cold temperatures. Our extension of the formalism to three dimensions shows that this approach is not quite accurate, because it ignores the OHT associated with overlapping circulations that span the same temperature classes, i.e. the *mixed* overturning circulations that we define below. While the contribution of mixed cells is possibly small in the idealized study of Vallis and Farneti, it is crucial for studies of the observed ocean heat transport especially in the North Atlantic.

b. Heatfunction in three dimensions

Numerous studies have proceeded to integrate the complex three-dimensional oceanic and atmospheric circulations in density coordinates in order to obtain a description of the overturning circulation (e.g. Andrews 1983; Nurser and Lee 2006). The overturning circulation in temperature coordinates is defined analogously, but for the change of averaging coordinate (e.g. Saenko and Merryfield 2006; Czaja and Marshall 2006). Here we wish to show how this overturning circulation is related to the OHT. Consider a zonal slice of ocean at a fixed latitude y, that is an $x-z$ section through the ocean. We define $A(y,\theta,t)$ as the area of that section below a certain potential temperature θ,

$$A(y,\theta,t) = \iint_{\theta' \leq \theta} \mathrm{d}x\mathrm{d}z. \tag{2}$$

The area $A(y,\theta,t)$ can be changed either by horizontal advection of water colder than θ, or by diabatic heating and cooling, i.e. it satisfies the conservation equation (see Nurser and Lee 2006, for a detailed derivation of this equation),

$$\frac{\partial A}{\partial t} = -\frac{\partial}{\partial y}\iint_{\theta' \leq \theta} v \ \mathrm{d}x\mathrm{d}z - \frac{1}{\rho_0 c_p}\frac{\partial}{\partial \theta}\iint_{\theta' \leq \theta} \mathcal{D} \ \mathrm{d}x\mathrm{d}z, \tag{3}$$

where v is the meridional velocity and $\mathcal{D}$ includes all processes that irreversibly modify the potential temperature of the fluid,

$$\rho_0 c_p \frac{D\theta}{Dt} = \mathcal{D}. \tag{4}$$

Eq. (3) ignores any evaporation and precipitation at the ocean surface. Addition of these terms is

discussed in Appendix A.

Taking a long-time average of Eq. (3) to eliminate time dependence (assuming that on long times the system is in equilibrium), the equation for the time-averaged $\bar{A}(y)$ becomes,

$$\frac{\partial \Psi}{\partial y} + \frac{1}{\rho_0 c_p}\frac{\partial D}{\partial \theta} = 0, \tag{5}$$

where we introduced the function Ψ to represent the total horizontal transport below a θ-surface and D for the total diabatic heating below the same surface,

$$\Psi(y,\theta) = \overline{\iint_{\theta' \le \theta} v \; \mathrm{d}x\mathrm{d}z}, \qquad D(y,\theta) = \overline{\iint_{\theta' \le \theta} \mathcal{D} \; \mathrm{d}x\mathrm{d}z} \tag{6}$$

and the overbars denote long-time averages. It can be shown that the function Ψ is the streamfunction associated with the zonally averaged mass flux in temperature coordinates (Nurser and Lee 2006): the transport of fluid with temperature between θ and $\theta + \Delta\theta$ is $(\Delta\Psi/\Delta\theta)\ \Delta\theta$ and hence the streamfunction's isothermal derivative, $\partial\Psi/\partial\theta$, gives the meridional transport along an isotherm. The streamfunction Ψ differs in one important respect from the streamfunction in z-coordinates, in that it includes contributions both from the zonal mean flow and from eddy motions generating correlations between temperature layer thickness and velocity (eddy motions are defined as departures from a zonal and temporal mean). Thus Ψ describes the mass transport by both the zonally averaged flow and the bolus flow due to eddy motions, i.e. it is the θ-coordinates representation of the residual overturning streamfunction used in atmospheric and oceanographic studies (Andrews 1983).

Eq. (5) states that the y-divergence of the meridional mass transport is balanced by the θ-divergence of the diapycnal flux D. We can introduce a *heatfunction* $H(y,\theta)$ as,

$$\rho_0 c_p \Psi \equiv \frac{\partial H}{\partial \theta}, \qquad D \equiv -\frac{\partial H}{\partial y}. \tag{7}$$

The heatfunction so defined represents the pathways of heat throughout the ocean in (y,θ) space associated with the streamfunction $\Psi(y,\theta)$. We can show that H describes how heat is moved around the ocean in response to irreversible diabatic heating and cooling. Let us integrate Eq. (7)

and Eq. (5) over a region $\mathcal{R}(y,\theta)$ composed of waters colder than θ and confined between a latitude y and the northern edge of the ocean (shaded area in Fig. 1a),

$$H(y,\theta) \equiv \int_{\theta_B}^{\theta} \rho_0 c_p \Psi(y,\theta)\ \mathrm{d}\theta = -\overline{\iiint_{\mathcal{R}(y,\theta)} \mathcal{D}\ \mathrm{d}x\mathrm{d}y\mathrm{d}z}, \tag{8}$$

where θ_B is the temperature of waters at the ocean bottom. The heatfunction $H(y,\theta)$ represents the northward transport of heat across a latitude y and below a temperature θ. This advective OHT is balanced by the diabatic heat input in the whole region $\mathcal{R}(y,\theta)$ as sketched in Fig. 1a. Hence the heatfunction describes the northward heat flux driven by diabatic heating and cooling. Any closed circulation exchanging waters at the same temperature is automatically filtered out, because it is not associated with diabatic heat gain. Finally the value of the heatfunction $H(y,\theta)$ at the ocean surface is equal to the sum of the surface heat flux north of y and any lateral diffusion across the zonal slice of ocean at y.

FIG. 1

A major goal of this paper is to quantify the OHT by individual branches of the overturning ocean circulation. Heatlines, lines of constant H, often span more than one overturning streamfunction loop, especially close to the ocean surface where different circulations overlap. One can estimate the OHT by individual branches of the circulation using a combination of heatfunction and streamfunction. Consider the circulation defined by a closed streamline contour in Fig. 1b. A closed circulation transports zero mass across any latitude y, but it transports heat because the northward flowing waters have different temperatures than those flowing southward. The temperature change results from the diabatic heating the waters experience as they flow along the streamline loops. This balance is expressed quantitatively by integrating Eq. (5) over the region $\mathcal{R}(y,\theta)$ enclosed by the latitude y to the south and the closed streamline contour to the north (see Fig. 1b),

$$OHT(y,\theta_u,\theta_l) = \int_{\theta_l}^{\theta_u} \rho_0 c_p \left(\Psi(y,\theta) - \Psi(y,\theta_l)\right)\ \mathrm{d}\theta = -\overline{\iiint_{\mathcal{R}(y,\theta)} \mathcal{D}\ \mathrm{d}x\mathrm{d}y\mathrm{d}z}. \tag{9}$$

The temperatures θ_u and θ_l are the maximum and minimum temperatures reached by the closed circulation at the latitude y. The term $\rho_0 \left(\Psi(y,\theta) - \Psi(y,\theta_l)\right)$ is the meridional mass transport

between θ and θ_l: Eq. (9) states that the OHT associated with an overturning circulation is proportional to the mass transported by that circulation times the temperature difference it encounters as pointed out by Czaja and Marshall (2006).

We can now use (9) to express the meridional OHT due to a closed circulation in terms of the heatfunction and streamfunction,

$$OHT(y, \theta_u, \theta_l) = H(y, \theta_u) - H(y, \theta_l) - \rho_0 c_p \Psi(y, \theta_l) \, (\theta_u - \theta_l) \, . \tag{10}$$

For a closed and isolated circulation, defined by a zero streamline contour $\Psi(y, \theta_l) = 0$, the meridional OHT is given by the difference between the values of heatfunction at the coldest and warmest temperatures spun by that circulation at y (Fig. 1b). For circulations embedded in other flows, like that shown in Fig. 1c, one must further subtract the OHT by the surrounding flow, $\rho_0 c_p \Psi(y, \theta_l) \, (\theta_u - \theta_l)$.

It is instructive to apply the heatfunction formalism to some idealized flows. Consider the three global ocean circulations sketched in Fig. 2. In the first panel, we have two isolated cells at warm temperatures, while in the second panel we have an isolated cell at cold temperatures. The OHT associated with each of those circulations is easily estimated by computing the difference in $H(y, \theta)$ between the top and bottom of the circulations at each latitude. The situation is a bit more complicated for the circulation depicted in the third panel, which is simply the sum of the circulations in the first two panels. In the northern hemisphere the warm and cold cells appear to be connected through a circulation that spans the full ocean depth, much alike in the North Atlantic (see the third panel of Fig. 3 below). There is a particular contour Ψ_{mixed} that separates the core of the warm and cold overturning cells. We can therefore estimate separately the OHT by the warm and cold circulations applying Eq. (10) with θ_l being the temperature that separates the two cells. We can also estimate the global OHT by the full overturning circulation in the northern hemisphere. This second estimate will be larger than the sum of the heat transported by the warm and cold cells, because it includes the contribution by the circulation spanning the whole ocean depth (see Fig. 2). This contribution, which we call the *mixed mode*, cannot be ascribed to surface

or abyssal circulation without additional information. Much of the debate on whether the OHT is more sensitive to surface or abyssal circulations is due to situations such as this, where there is no complete separation between shallow and deep circulations in a zonally averaged sense. In this paper we will use a suite of numerical simulations to determine whether the portion of the OHT due to mixed modes spanning the whole ocean depth is more sensitive to surface or abyssal forcing.

FIG. 2

The focus of this paper is on the OHT. However a *tracer-function* can be defined for any oceanic tracer by replacing θ with the tracer considered and the heat equation (4) with the appropriate tracer equation. We made no assumption on the form of the term $\mathcal{D}$ in the rhs of Eq. (4); this term can include sources and sinks of tracers or reaction with other tracers. Hence a tracer-function can be defined for any chemical or biological tracer to describe its pathways in a zonally averaged sense. Addition of sources and sinks at the surface through air-sea fluxes is discussed in Appendix A.

The definition of heatfunction used in this paper is related to those introduced by Boccaletti et al. (2005) and Greatbatch and Zhai (2007). Boccaletti et al. (2005) start from the time and zonally averaged heat equation in (y, z) space,

$$\nabla \cdot \langle \boldsymbol{u}\theta - \kappa \nabla \theta \rangle = 0, \tag{11}$$

obtained from Eq. (4) by setting $\mathcal{D} = \rho_0 c_p \nabla \cdot \kappa \nabla \theta$ (the angle brackets denote both zonal and temporal average). This budget states that the sum of the advective and diffusive heat fluxes has zero divergence. It is therefore possible to represent the heat fluxes in terms of a heatfunction ϕ defined as $\partial_z \phi = \rho_0 c_p \langle v\theta - \kappa \partial_y \theta \rangle$ and $\partial_y \phi = -\rho_0 c_p \langle w\theta - \kappa \partial_z \theta \rangle$. This definition is, however, dominated by the advective heat flux associated with the recirculation of waters at constant temperature which do not contribute to the vertically integrated OHT. Boccaletti et al. (2005) show that these inconsequential advective heat fluxes can be eliminated in the definition of the heatfunction by subtracting from θ the mean temperature along a streamline. Greatbatch and Zhai (2007) show that, more generally, one can define ϕ by integrating the heat flux along zonal mean temper-

atures. This problem does not arise when averages are taken at constant temperature, because the averaging filters out any recirculation at constant temperature. Eq. (5) shows that the circulation Ψ is forced by diabatic heating, i.e. it includes only circulations that cross isotherms.

There are two important differences between the heatfunction used in this paper and the definitions in Boccaletti et al. (2005) and Greatbatch and Zhai (2007). First, the heatfunction defined in (7) represents the pathways of heat transported by the ocean circulation, while the previous definitions included both advective and diffusive heat transports. The difference is very small for the real ocean, where heat transport by advective processes dominates over diffusion. However in numerical models heat transport by diffusive parameterizations can be substantial. Our focus here is on diagnosing heat transport by different branches of the overturning circulation and the present definition is more appropriate. Second, the definition in Eq. (5) can be extended to non-conservative tracers which have sources and sinks.

3. Numerical Model and the Mass Transport Streamfunction

The heatfunction approach will now be used to study what processes control the OHT in a numerical model of the ocean. The numerical experiments are carried out with the MIT general circulation model (Marshall et al. 1997a,b). The model has a horizontal resolution of 2.8° and 15 levels in the vertical. The geometry is 'realistic' except for the absence of the Arctic Ocean; bathymetry is represented with shaved cells (Adcroft et al. 1997). The model is forced by observed monthly mean climatological surface wind stresses from Trenberth and Olson (1990). The surface heat and freshwater fluxes are each the sum of two terms: (1) imposed monthly mean climatological heat fluxes and annual mean evaporation-precipitation (Jiang et al. 1999), and (2) restoring toward observed monthly mean climatological temperature and salinity (Levitus et al. 1994) with time scales of 2 and 3 months, respectively. Freshwater fluxes are imposed as virtual salt fluxes in the salinity equation. The model is therefore capable of modifying its heat and salt fluxes in response to changes in the circulation. No representation of sea-ice is included. All simulations

are initialized from Levitus climatology and run until they reach equilibrium after 7000 years (the only exception is the "water hosing" experiment described below where equilibrium was reached in 2500 years). All statistics are computed from the last year of integration from monthly mean outputs (the model has a seasonal cycle, but no interannual variability).

At the coarse resolution used in this study, processes such as convection (Marshall and Schott 1999), mixing (Ledwell et al. 1993), and transfer of properties by the mesoscale eddy field (Gent and McWilliams 1990) are subgridscale and must be parameterized. Convection is parameterized by enhanced vertical diffusion whenever the water column becomes statically unstable. Mixing is represented with eddy viscosities and diffusivities. The horizontal and vertical viscosity are set to 5.0×10^{5} m^2 s^{-1} and 1.0×10^{-3} m^2 s^{-1}, respectively. There is no explicit horizontal diffusivity. The vertical diffusivity is one of the parameters that are varied across simulations. It is set to 0.3×10^{-4} m^2 s^{-1} in the control run. The phyisics of mesoscale eddies is parameterized with an eddy-induced transport (Gent and McWilliams 1990) and an isopycnal diffusivity (Redi 1982). Tapering of isopycnal slopes is done adiabatically using the scheme of Gerdes et al. (1991). Both thickness and isopycnal diffusion coefficients are set to 1000 m^2 s^{-1}.

The model reproduces most of the features commonly associated with the large-scale ocean circulation: the equatorial current system, the wind-driven gyres at mid-latitudes, the Antarctic Circumpolar Current in the Southern Ocean, and the formation of deep waters at high latitudes (see Ferreira and Marshall 2006). For present purposes, we are interested in the overturning circulation produced by the model. In Fig. 3 (left), we show the traditional overturning streamfunction for the global ocean in z coordinates,

$$\psi_{eul}(y,z) = \overline{\int\int_{z=-H}^{0} v \; \mathrm{d}x\mathrm{d}z}, \tag{12}$$

where z=-H is the ocean bottom and the overbar represents a one-year time average. The model reproduces the shallow wind-driven overturning circulations in each hemisphere, divided into tropical and subtropical cells, whose structure in the horizontal constitutes the familiar wind-driven tropical and subtropical gyres. There are also overturning circulations associated with

high-latitude convection and abyssal mixing, which constitute the bulk of the circulation residing below the thermocline. In the Southern Ocean, a strong Deacon cell reflects the circulation driven by the southern hemisphere westerlies.

In Fig. 3 (middle), we show the residual overturning circulation, i.e. the overturning circulation associated with the full meridional mass transport given by the sum of the Eulerian meridional velocity, v, and the eddy-induced velocity parameterized with the Gent-McWilliams scheme, v_{GM}:

$$\psi_{res}(y,z) = \overline{\iint_{z=-H}^{0} (v + v_{GM}) \ \mathrm{d}x\mathrm{d}z}. \tag{13}$$

McDougall and McIntosh (2001) refer to the eddy-driven transport as a quasi-Stokes drift for finite amplitude eddies. The residual streamfunction is therefore the sum of the Eulerian and quasi-Stokes transports and approximates a Lagrangian streamfunction, i.e. the streamfunction associated with transport of tracers like temperature (e.g. McDougall and McIntosh 2001; Plumb and Ferrari 2005). The only substantial difference between the Eulerian and the residual streamfunctions shows up in the Southern Ocean. The Deacon cell vanishes in the residual picture, because mesoscale eddies drive an anticlockwise circulation that largely cancels the mean Ekman circulation (e.g. Karsten and Marshall 2002).

In the residual framework, the abyssal circulation is characterized by two deep overturning circulations of magnitude similar to the two surface circulations. The northern hemisphere overturning associated with NADW formation is confined between the surface cells and 2000 m, it contributes just under half of the meridional mass transport at mid-latitudes and dominates north of 50°N. Below 2000 m, the circulation is dominated by an anticlockwise circulation with a maximum transport of 8 Sv, representing the penetration of Antarctic Bottom Water (AABW). When considering individual basins, we find that in the Atlantic the deep overturning circulation reaches a maximum of 15 Sv, while the surface wind-driven overturnings are somewhat smaller, barely reaching 10 Sv. In the Pacific, the overturning circulation is largely anti-symmetric about the equator and it is almost entirely associated with the Ekman flows generated by the surface winds. These circulations carry between 15 and 20 Sv in each hemisphere.

In Fig. 3 (right), we show the overturning circulation in temperature space introduced in sec. 2,

$$\Psi(y,\theta) = \overline{\iint_{\theta_B}^{\theta} (v + v_{GM}) \ \mathrm{d}x\mathrm{d}z}, \tag{14}$$

where $\theta(x,y,z)$ is a two-dimensional isothermal surface and $\theta_B = \theta(x,y,-H)$ is the temperature at the bottom of the ocean. Details of the calculation are given in Appendix B. We use the sum of the mean and eddy-induced velocities in the definition of streamfunction in temperature space, because the model advects temperature with the sum of the two. (In an eddy resolving model the eddy-induced contribution v_{GM} would arise from temporal correlations between v and fluctuations in the temperature surface θ). Notice however that the definition in (13) includes only the eddy-contribution due to the Gent-McWilliams scheme, while the definition in (14) includes the additional contribution of correlations between v and θ due to time-mean departures from the zonal mean, the so-called 'standing eddies'. One can modify the definition in (13) to include contributions by standing eddies, but the actual computation is very noisy.

The mass transport in temperature coordinates shows that the shallow overturning circulations associated with the wind-driven gyres span the large temperature gradient associated with the ocean thermoclines, while the deep and abyssal circulations span cold waters with small temperature contrasts. In the previous section we have shown that the OHT associated with an overturning circulation is proportional to the strength of that circulation multiplied by the temperature difference it encounters ($\rho_0 c_p \Psi \ \Delta\theta$). The shallow and deep circulations have comparable strengths, but the shallow ones are better positioned to transport heat because of the large $\Delta\theta$ they span. The separation between shallow and deep circulations holds well in the southern hemisphere. In the northern hemisphere, instead, the two circulations partly overlap and a clear partitioning of OHT requires a careful application of the heatfunction formalism as discussed in the next section.

FIG. 3

4. Vertical structure of the heat transport

a. Global heat transport

The traditional way to diagnose the OHT is to compute the vertical integral of the temperature flux $\rho_0 c_p v\theta$ across an east-west section bounded by continents (Hall and Bryden 1982). This ensures that, as long as the total mass flux across the section is zero, the OHT is due to water flowing northward at one temperature and returning southward at a different temperature. In Fig. 4 we show the vertically integrated OHT in each ocean and the total transport summed over all oceans as produced by the numerical model. The global OHT peaks at about 20° latitude, with maxima of 1.2 PW (1 PW=10^{15} W) in the southern hemisphere and 1.3 PW in the northern hemisphere. The model captures the differences in OHT among different ocean basins: heat is transported northward at all latitudes in the Atlantic basin and poleward in both hemispheres in the Indo-Pacific basin. It also reproduces well the observed OHT in the Indo-Pacific, but it underestimates the observed OHT in the Atlantic by nearly 30%. This bias is associated with too cold a Gulf Stream core and too warm a deep undercurrent core compared to observations (not shown): the model is too coarse to capture the full OHT associated with boundary currents which are barely resolved. Similar biases are found in most coarse resolution ocean models used for climate studies (Jia 2003). Our goal is to quantify the sensitivity of OHT to changes in different branches of the overturning circulation, so the absolute value of OHT is less of a concern. However the model deficiency in reproducing some components of the OHT becomes an issue when extrapolating our results to the real ocean.

FIG. 4

In order to identify the pathways of the heat transported by the ocean circulation, we compute the heatfunction defined in (7). The calculation is straightforward: one integrates with respect to θ the streamfunction shown in Fig. 5a. The heatfunction is defined positive (negative) for heat moving northward (southward). The contours of constant heatfunction show heat flowing from the atmosphere into the ocean at low latitudes and coming back to the surface at higher latitudes. The topmost value of $H(y,\theta)$ equals the vertically integrated advective OHT, i.e. the total OHT minus the heat diffused across the latitude y by the Redi diffusion which parameterizes eddy transport of

heat along isopycnals (Redi diffusion is significant only in the Southern Ocean). Regions where the heatfunction is zero do not contribute any OHT. A comparison of panels (a) and (b) of Fig. 5 shows that the pathways of mass, represented by the streamfunction, are very different from the pathways of heat, represented by the heatfunction: the pathways of heat are set both by the mass transport and by the air-sea fluxes. This difference calls into question the paradigm of a global conveyor (Broeker 1991) to describe the ocean circulation and its impact on climate. Each oceanic tracer follows different pathways in a zonally integrated picture as a result of the different sources and sinks, even though all tracers are transported by the same three dimensional velocity field. A conceptual model of the OHT based on the mass streamfunction is clearly misleading.

FIG. 5

The heatfunction in Fig. 5b is surface intensified with a maximum OHT of 1.3 PW at the surface and no contribution to the OHT below 5°C corresponding approximately to 2000 m. Virtually all of the OHT in the southern hemisphere is achieved by a circulation warmer than 10°C confined to the upper 500 m; the abyssal circulation associated with AABW disappears in the heatfunction picture. In the northern hemisphere the heatfunction penetrates deeper, because there are contributions from a shallow warm cell and a deeper cold circulation associated with NADW. The heatfunction is confined between 50°N and 50°S–the OHT vanishes poleward of 50 degrees. Heat travels along continuous pathways that connect the midlatitude subduction sites to regions of equatorial upwelling. Note that there is no reduction in OHT in the latitude band straddling the separation between the tropical and subtropical gyres; heat must be transported by the parameterized transient eddies across these latitudes, i.e. the eddy-induced transport.

The slope of streamlines in latitude-temperature space provides useful information on the ocean heat budget. The warm overturning cells are strongly tilted, i.e. they change temperature as they move across latitudes, suggesting that they are exposed to strong diabatic heating and cooling at all latitudes as per Eq. (5). The dashed lines in Fig. 5a show the mean and coldest temperatures found at the surface at a particular latitude. The warm overturning cells are mostly confined to temperature classes that are entrained in the surface mixed layer every winter and are directly exposed to surface fluxes. The deep overturning cells, once they plunge in the ocean inte-

rior, are nearly horizontal in latitude-temperature space, because interior diffusion of heat is very weak and the overturning streamlines do not drift significantly across temperature classes.

Using Eq. (10), we can compute the OHT associated with each of the four closed circulations that describe the mass transport in the zonal average (see Fig. 5a). In the southern hemisphere the shallow warm circulation accounts for nearly all of the OHT as shown in Fig. 5c (dashed black) with weak, and opposing, contributions from the cold circulations associated with NADW (dashed grey) and AABW (solid grey). In the northern hemisphere the shallow and deep circulations overlap and cannot be fully separated. Choosing the 11.5 Sv streamline as the separatrix between the two circulations, we estimate a peak OHT of 0.3 PW for the warm cell (dashed black) and a peak OHT of 0.05 PW for the cold cell (solid grey). The heat transported by these two cells falls short of the total advective OHT peaking at 1.3 PW: most of the OHT cannot be ascribed to either circulation separately and is due to the superposition of the two circulations, the mixed mode (dashed grey). The difficulty in partitioning the OHT among the various overturning circulations has generated a vigorous discussion on the relative roles of shallow and deep circulations in transporting heat. Here we tackle the question with a series of sensitivity studies where we change the strength of the various circulations and compute their impact on the heatfunction and the associated OHT.

b. Atlantic Heat Transport

It is often argued that the OHT in the Atlantic is primarily associated with a deep meridional overturning circulation that results from NADW formation at high northern latitudes (Hall and Bryden 1982). The argument goes that the deep circulation dominates the OHT because it flows poleward at the surface and equatorward at depth, therefore encountering a large top to bottom vertical temperature difference. This is supposedly in opposition to the horizontal transport in wind-driven gyres which have a meridional overturning comparable to the deep circulation, but span the much smaller east-west temperature difference.

The streamfunction for the Atlantic is shown in Fig. 6a. Boccaletti et al. (2005) show that

the traditional decomposition into horizontal and vertical OHT[1] used for example by Bryden and Imawaki (2001) assigns, at $24°$N, less than 0.1 PW to the horizontal circulation and 0.8 PW to the vertical circulation. The overturning circulation in latitude-depth space is indeed dominated by the deep flow of NADW flowing into the abyss. The prevailing interpretation is that this deep circulation carries the 0.8 PW and hence dominates the OHT (Bryden and Imawaki 2001). However, Fig. 6b shows that the OHT is surface intensified and it is the result of a circulation spanning both warm and cold temperature classes (Fig. 6a). Fig. 6c confirms that the closed warm and cold circulations account for a minuscule fraction of the OHT. Approximately 75% of heat is carried by a larger cell enclosing both circulations which is likely sensitive to both high latitude convection and to subtropical winds.

FIG. 6

Talley (2003) has recently attempted a careful partitioning of OHT from observations. She found that the shallow circulation contributes a large fraction of the OHT in the North Atlantic. Talley assumed that the wind-driven OHT is carried by a closed circulation confined to waters lighter than 27.3 kg m^{-3}, the maximum winter surface density for the North Atlantic subtropical subduction region. She estimated that 13 Sv are transported southward in the gyre interior and returned northward in the Gulf Stream. The associated OHT remained quite uncertain and ranged between 0.4 to 0.1 PW, depending on whether the bulk of the northward transport occurred in the warmest core of the Gulf Stream or whether it was spread uniformly over the whole Gulf Stream layer. We repeated the same calculation with the model output and we obtained OHTs of 0.5 and 0.2 PW depending on the choice of return temperature in the Gulf Stream, values very close to

[1]For any latitude y, the meridional velocity v and temperature θ are separated into zonally averaged baroclinic values, $\langle v\rangle(z)$ and $\langle\theta\rangle(z)$, and deviations from the zonal averages, $v'(x,z)$ and $\theta'(x,z)$. The OHT can then be broken up into two components,

$$OHT(y) = \int \rho_0 c_p \langle v\rangle\langle\theta\rangle L(z)\mathrm{d}z + \iint \rho_0 c_p v'\theta'\mathrm{d}x\mathrm{d}z, \tag{15}$$

where $L(z)$ is the width of the section at each depth. The vertical component (first term) is interpreted as the OHT associated with abyssal circulations because it is associated with a vertical overturning circulation. The residual (second term), instead, is interpreted as the contribution of the horizontal wind-driven gyres.

those found by Talley. We conclude that the bulk of the OHT in the Atlantic cannot be uniquely ascribed to shallow or deep circulations. Alternatively we will ask how sensitive is the OHT to changes in winds versus changes in mixing and air-sea fluxes.

c. Indo-Pacific Heat Transport

The heat budget of the Indo-Pacific basin is simpler to analyze, because the surface and deep circulations are well separated in temperature space and there is no ambiguity in partitioning the OHT. Fig. 7b shows that the heatfunction, and hence the OHT, are confined to the upper ocean with hardly any contribution from deep circulations. The northern hemisphere surface cell transports 0.5 PW poleward in the upper 400 m, while the southern hemisphere cell transports almost 0.8 PW poleward in the upper 700 m. The OHT in the southern hemisphere involves also a deeper circulation connected to the Southern Ocean which contributes less than 0.1 PW. These estimates are consistent with the observational results of Ganachaud and Wunsch (2003) and Talley (2003). FIG. 7

5. Physical processes controlling the ocean heat transport

The heatfunction for the global ocean in Fig. 5 shows that a large fraction of the OHT is carried by surface circulations in the tropical and subtropical thermoclines, with an additional contribution from the deep circulation associated with NADW. This suggests that the OHT is more sensitive to the processes that drive the shallow circulations and less to the processes that drive the deep and abyssal circulations. While the effect of surface forcing and interior mixing on the overturning streamfunction has been previously documented in the literature (e.g. Vallis 2000; Saenko and Merryfield 2005; Ito and Marshall 2008), their effect on OHT is quite different as we illustrate below with a suite of sensitive experiments.

a. Abyssal mixing

The importance of the deep overturning circulation in transporting heat is often invoked to motivate the study of abyssal mixing in the ocean (e.g. Jayne et al. 2004). The argument goes that the OHT is limited by the ability of the ocean to mix dense bottom waters across the stratification of the abyss (e.g. Munk and Armi 2001). However Fig. 5 shows that the OHT is largely confined to the upper ocean away from the abyssal stratification. Studies of deep abyssal mixing should be seen in this context. The mass transport is sensitive to mixing, but the OHT in addition depends on the temperature difference, which is small in the abyss (Boccaletti et al. 2005).

First we compare the changes in mass and heat transport between a simulation with a constant diapycnal mixing coefficient of κ=0.3$\times 10^{-4}$ m^2 s^{-1} (the control run) and a simulation with κ=0.3$\times 10^{-4}$ m^2 s^{-1} in the upper 2000 m and κ=1.7$\times 10^{-4}$ m^2 s^{-1} below (Bryan and Lewis 1979). The Bryan and Lewis profile is a crude attempt to include basic features of the vertical profile of κ observed in the real ocean. Measurements find that mixing is weak and uniform in the upper ocean (Ledwell et al. 1993), while it is enhanced in the abyss where topographic waves radiate from bottom topography and break (Polzin et al. 1997; Garabato et al. 2004). We set the abyssal value of diapycnal mixing to 1.7$\times 10^{-4}$ m^2 s^{-1} so that the volume averaged κ for the full ocean is close to 1.0$\times 10^{-4}$ m^2 s^{-1}, a value consistent with tracer budget estimates for the global ocean (e.g. Wunsch and Ferrari 2004). This simulation with an enhanced bottom mixing is arguably our most "realistic" experiment.

Fig. 8 shows the volume transport for the simulation with the Bryan and Lewis diapycnal mixing profile. The abyssal circulation more than doubles in response to the enhanced abyssal mixing, going from about 9 Sv in the control run with a uniform κ to 21 Sv (Fig. 8). However the heat transport remains virtually unchanged (compare Fig. 5 and Fig. 8), because there is hardly any OHT below 2000 m where κ is enhanced. Notice that the model is, in principle, free to adjust its surface heat flux in response to changes in the circulation. We conclude that the abyssal overturning circulation and stratification are indeed controlled by abyssal mixing, but the modeled

OHT is not (see also Scott and Marotzke 2002).

Saenko and Merryfield (2005) studied extensively the effect of abyssal mixing on the circulation of an ocean model. They used a parameterization of abyssal mixing which included modulations by topographic roughness and by the intensity of bottom flows. Consistent with our results, they found that the enhanced abyssal diffusivity led to increased bottom water circulation and deep stratification, especially in the Pacific. However, the OHT was unaffected by the abyssal circulations because stratification is too weak below 2000 m.

Our result that abyssal mixing has little effect on heat transport seems at odds with a recent paper by Simmons et al. (2004), who performed a study similar to that of Saenko and Merryfield but came to the opposite conclusion that abyssal mixing can substantially modify the transport of heat. In reality there is no contradiction between their result and ours: Simmons and collaborators compared a run with a constant diffusivity with one in which the thermocline diffusivity was reduced and the abyssal one was increased. They attributed the difference in heat transport between the two runs to changes in abyssal mixing. However, as we show in the next section, heat transport is very sensitive to upper ocean processes and the difference in OHT between the two runs was likely due to the different mixing rates in the thermocline. FIG. 8

b. Thermocline mixing

We now consider the circulation and heat transport resulting from an increase of κ throughout the whole water column, as opposed to the bottom-confined increase considered in the previous section. The diapycnal mixing coefficient is increased uniformly to $\kappa = 1.0 \times 10^{-4}$ m^2 s^{-1}, a value three times larger than in the control run. Fig. 9 shows that increasing κ results in a doubling of the peak heat transport in the southern hemisphere (from 1.1 to 2.2 PW) and a smaller 0.2 PW increase in the northern hemisphere, i.e. a 15% increase. Hence mixing does affect the ocean heat budget when κ is increased throughout the whole water column, but not when κ is enhanced only below 2000 m. FIG. 9

A decomposition of the heat transport among closed circulations confined to the upper ocean (*warm cells*), closed circulations outcropping at high latitudes (*cold cells*) , and *mixed cells* flowing around the first two illustrates why the OHT is sensitive to where mixing is enhanced. At the scaling level, one can write the heatfunction as the sum of three terms representing each circulation – see Eq. (9):

$$\begin{aligned} H &= H_{warm} + H_{cold} + H_{mixed} \\ &\approx \rho_0 c_p \left[(\Psi_{warm} - \Psi_{mixed}) \Delta\theta_{warm} + (\Psi_{cold} - \Psi_{mixed}) \Delta\theta_{cold} + \Psi_{mixed} \Delta\theta_{mixed} \right] \quad (16) \end{aligned}$$

where Ψ_{warm} and Ψ_{cold} represent the magnitude of the warm and cold overturning cells, Ψ_{mixed} the value of the streamline separating the warm and cold cells, while $\Delta\theta_{warm}$, $\Delta\theta_{cold}$, and $\Delta\theta_{mixed}$ are the temperature contrasts spun by each circulation. A comparison of the bottom panels in Fig. 5 (the control run) and Fig. 9 (the run with $\kappa = 1{\times}10^{-4}$m^2 s^{-1}) shows that in the northern hemisphere the small increase in OHT is primarily associated with an increase in H_{warm}: the shallow overturning circulation strengthens in response to the increase in κ (Vallis 2006). In the southern hemisphere, instead, the large increase in OHT is associated with the appearance of a mixed mode, i.e. a circulation encircling both the shallow and deep circulations: H_{mixed} grows from $\sim$0.1 PW to $\sim$1 PW. The mixed mode represents waters upwelling from the abyssal Southern Ocean into the Pacific thermocline (Fig. 10). The upwelling results from the balance $w\partial_z\theta \approx \kappa\partial_{zz}\theta$ and results into $\Psi_{mixed} \approx 10$ Sv of waters raising from the abyss into the surface midlatitude waters and spanning a $\Delta\theta_{mixed} \approx 25$°C. This gives $H_{mixed} \approx \rho_0 c_p \Psi_{mixed} \Delta\theta_{mixed}$ $\approx$1 PW of additional heat transport.

FIG. 10

To further investigate the impact of diabatic mixing on the OHT in the southern hemisphere, we run four different simulations with uniform diffusivities of κ=(0.2,0.3,0.5,1.0)$\times10^{-4}$ m^2 s^{-1}. In Fig. 11, we report the maximum heatfunction associated with warm, cold and mixed circulations in the southern hemisphere from each of the four simulations. As κ is increased above $0.3{\times}10^{-4}$ m^2 s^{-1}, a mixed circulation develops and carries a growing OHT. In contrast the shallow and abyssal circulations decrease with κ, because increasing κ connects a progressively larger

fraction of the two separate circulations which become part of the mixed one. FIG. 11

These simulations show that diabatic mixing contributes a substantial heat transport when it acts in the upper ocean, but not when it is confined to the abyss. Mixing is particularly effective at transporting heat if it is increased at the base of the midlatitude thermoclines (which corresponds to the base of the shallow circulations), because it drives upwelling of abyssal waters towards the ocean surface. This generates an overturning circulation spanning the whole $\Delta\theta$ between cold abyssal waters and warm surface waters and drives a large OHT. While this is an interesting theoretical result, direct measurements argue against values of $\kappa > 0.3\times10^{-4}$ m^{2}s^{-1} at the base of the ocean thermoclines and hence diabatic mixing does not appear to play a major role in the ocean heat budget. An important implication of this analysis is that, contrary to the claim by Simmons et al. (2004), among others, tidally-driven mixing is unlikely to drive a significant OHT because it is largely confined to the abyss.

c. High latitude convection

The traditional view divides the oceanic circulation in a deep overturning connected to high latitude convection, and a shallow overturning driven by subtropical winds. Countless water-hosing experiments have illustrated the effect of shutting off the NADW formation on the OHT: once convection is shut off the Atlantic overturning ceases to transport heat poleward, resulting in high-latitude cooling (e.g. Bryan 1986). This result has prompted a vast literature on the role of convection in the North Atlantic on climate change (e.g. Rahmstorf 2002). However the impact of this shut off on the Earth's climate depends critically on what fraction of the OHT is associated with the deep overturning circulation and whether this circulation is only sensitive to freshwater fluxes or also to other forcing like winds. We tackle the first question here and address the role of winds in the next section.

The heatfunction analysis suggests that the bulk of the OHT in the North Atlantic is associated with a mixed circulation that transports warm waters northward at the surface and cold waters

southward in the abyss (H_{mixed} in Fig. 6c, dashed grey). A deep cell associated with high latitude convection contributes only 10% of the OHT (H_{cold} in Fig. 6c, thick solid grey). To quantify what fraction of H_{mixed} is associated with high latitude convection, we run a sensitivity experiment in which deep water formation in the North Atlantic is suppressed. To achieve this, the North Atlantic surface waters are freshened by lowering the restoring sea surface salinity uniformly by 2 psu poleward of 50°N. This results into an unrealistically large perturbation of the salinity field, but our goal is to completely suppress high latitude convection. The simulation is started from the equilibrium state of the control run and reaches, after 2500 years, a new equilibrium in which there is no deep water formation – the high-latitude water columns remain stable even through wintertime.

In Fig. 12, we show the streamfunction and heatfunction for the water-hosing experiment. The mixed overturning circulation seen in the control run (Fig. 6a) is nearly absent in the water hosing experiment (Fig. 12a) as the water mass transformation in which it is involved disappeared (1.5 Sv versus 8.0 Sv in the control run). The cross-equatorial flow (and heat transport) also vanished. The weak (∼2 Sv) cell centered at (50°N, 10°C) can be attributed to the wind-driven subpolar gyre. The shallow subtropical circulation is relatively unaffected by the collapse of the mixed circulation. The disappearance of the mixed mode amounts to a drastic decrease of the Atlantic OHT from 0.8 PW down to 0.3 PW, a decrease of approximately ∼60%, still much less than implied by studies that assume that the bulk of the OHT in the North Atlantic is associated with high latitude convection (e.g. Bryden and Imawaki 2001; Quadfasel 2005; Kuhlbrodt et al. 2007).

FIG. 12

The goal of the present experiment is not to simulate a realistic Laurentian ice-sheep break-up or a climate change scenario, but rather to set up a benchmark with a complete shutdown of deep water mass formation in the northern hemisphere. That said, our results, albeit extreme, are very similar to those seen in traditional water-hosing experiments. Note that, differently from the usual procedure, we do not directly control the anomalous freshwater flux into the North Atlantic. The anomalous freshwater flux associated with the modified sea surface salinity restoring for the

region poleward of 50°N was as large as 3.6 Sv during an initial transient, but it settled to 0.05 Sv within a century. Hence, the implied change in hydrological cycle in the new equilibrium is rather small.

Finally, we ought to anticipate that changes in the deep overturning (and the associated mixed mode) are as sensitive to winds as to deep water formation (see next section). Hence the impact of ice melting on high latitude convection, OHT and climate must be assessed against the competing changes in the atmospheric hydrological cycle and wind patterns (see also Wunsch 2010). Previous water-hosing experiments focused on the effect of river runoff by ice melting and implicitly assumed that the atmospheric circulation, with its associated winds and freshwater fluxes, remained constant through radically different climates. This seems quite unlikely.

d. Wind stress

The final suite of sensitivity experiments focuses on the role of winds on the OHT. Wunsch and Ferrari (2004) show that the global ocean circulation is powered by surface winds and hence we expect a strong sensitivity of OHT to winds. A comprehensive study of the effect of winds on OHT should consider changes both in their magnitude and in their spatial patterns – the overturning circulation is sensitive to both the magnitude of the wind stress (e.g. Ekman flows) and its curl (e.g. Sverdrup flows). Such an endeavor is well beyond the scope of this paper. Our goal is simply to emphasize the strong sensitivity of OHT to surface winds, leaving the specifics to future work. We therefore run a series of simulations in all equal to the control run, but where the surface wind stress was multiplied by a constant factor. In this way the wind stress and its curl were varied by the same amount.

The impact of the surface wind stress on OHT has been documented in recent papers by Saenko and Weaver (2004) and Vallis and Farneti (2009). Our results are largely consistent with these previous works, but our emphasis is slightly different in that we wish to compare the impact of the surface wind stress to other processes affecting the OHT.

Fig. 13 shows the overturning streamfunction and heatfunction for the simulation where the magnitude of the wind stress is twice that in the control run, an increase probably larger than in any climate experienced by the Earth in the past. The shallow warm overturning circulations are much stronger than in the control run, as might be anticipated because these circulations represent the wind-driven gyres. Notice, however, that the mixed circulation, representing the circulation of NADW, has also dramatically increased. This is a result of the increase in the surface wind-driven gyres and in the deep circulation pulled by the wind-driven upwelling of waters in the Southern Ocean (e.g Toggweiller and Samuels 1995; Wofe and Cessi 2010). The abyssal cold circulations, instead, do not change much – in the model these circulations are primarily convective.

FIG. 13

The increase in shallow and mixed circulations results in close to a doubling of OHT. Note, again, that the increase occurs both in H_{warm} and in H_{mixed} (Fig. 13c). The main point here is that changes in winds drive changes in the heat transport associated with the deep circulations in the North Atlantic. High latitude convection is not the only process affecting this circulation and its associated OHT.

To better understand the scaling of the OHT with the wind stress, we run a suite of simulations where the wind stress was 0.5, 1.5 and 2 times the value used in the control run. The maximum value of the (global) streamfunction for the warm and cold circulations in the northern hemisphere are plotted in Fig. 14 (left) alongside with the value of the separatrix Ψ_{mixed} between the two cells. Both closed circulations and the separatrix scale linearly with the wind, i.e. $\Psi_{warm,cold,mixed} \propto \tau$. The temperature stratification hardly changes across these simulations, as it is strongly constrained by the same surface restoring. Therefore according to Eq. 16, the three heatfunction contributions, and hence the total OHT, also scale linearly with the wind $H_{warm,cold,mixed} \propto \tau$ – the cold cell remains pretty insignificant because of the small $\Delta\theta_{cold}$ it encounters. The heat transported by the warm and mixed mode cells grows from 0.1 to 0.8 PW and 0.8 to 1.4 PW, respectively. Taking $(\Psi_{warm} - \Psi_{mixed})$ and Ψ_{mixed} from Fig. 14, such heat transport variations require $\Delta\theta_{warm} \sim$6°C and $\Delta\theta_{mixed} \sim$22°C. These are reasonable estimates of the temperature contrasts spun by these circulations.

FIG. 14

Our results are consistent with those in Vallis and Farneti (2009). Vallis and Farneti using an idealized coupled ocean-atmosphere model showed that the OHT scales linearly with the surface winds if the ocean diabatic mixing is weak. We have shown that the OHT is only sensitive to mixing above 2000 m and mixing is typically weak in this upper part of the water column.

The linear dependence of the OHT on the winds for the deep circulations should be taken with caution. We argued that this scaling likely reflects the pulling by southern hemisphere westerlies. The upwelling of waters in the Southern Ocean is the result of a competition of wind- and eddy-driven circulations (e.g. Hallberg and Gnanadesikan 2006). In our simulations the eddy strength is parameterized with a constant eddy diffusivity and does not change with the winds. In contrast, high resolution simulations suggest that the eddy strength changes with winds in such a way as to offset changes in the wind-driven circulation. It is therefore likely that the sensitivity of the OHT to deep circulations is overestimated in our simulations. This is, however, of little importance for our conclusions that the OHT scales quasi-linearly with the surface winds–the bulk of the OHT is indeed associated with wind-driven subtropical overturning cells, which scale linearly with the surface winds. The deep circulations are less important for the overall scaling.

Our conclusion is twofold. First, the OHT is very sensitive to changes in winds, because a large fraction of this transport is associated with the wind-driven subtropical gyres. Second, the smaller fraction of global OHT associated with deep water formation in the North Atlantic and Ekman upwelling in the Southern Ocean is also sensitive to winds. Therefore the feedback of the oceans on climate must be understood in the context of what the corresponding changes in winds might have been. Water hosing experiments typically assume that the ocean response to massive ice melting is limited to a decrease in high latitude convection and its associated heat transport. However removal of large ice masses is likely to be accompanied by changes in atmospheric wind patterns, which in turn would induce changes in OHT. This conclusion is consistent with the increasing evidence that the wind-driven circulation and its coupling to the atmosphere is the largely unknown player in climate change (Held 2001).

6. Conclusions

The goal of this paper was to identify what physical processes drive the ocean heat transport. This is often done by diagnosing the meridional overturning circulation. We have shown that a more quantitative picture can be inferred from a new diagnostic, the *heatfunction*. The heatfunction is obtained by computing the heat transport associated with different branches of the overturning circulation in temperature coordinates. In the Pacific and Indian oceans, the heatfunction shows that the bulk of the heat transport is associated with tropical and subtropical wind-driven gyres, despite the presence of strong circulations in the abyss. In the Atlantic Ocean, instead, the heat transport is associated with an overturning circulation that spans both the thermocline waters associated with the wind gyres and the deep waters formed through high latitude convection. It is, however, erroneous to conclude that heat transport in the Atlantic Ocean is mostly sensitive to changes in high latitude buoyancy fluxes and Southern Ocean winds; in addition the heat transport is very sensitive to mid- and low-latitude winds.

While the importance of surface and deep circulations to ocean heat transport has been recognized in the past, the heatfunction provides a useful diagnostic to objectively quantify the various contributions. The heatfunction might prove very useful to test the skill of ocean models used for climate studies. The Earth's climate is very sensitive to ocean heat transport, but the diagnostics typically used offer little insight on the pathways of heat through models. Traditionally one looks at overturning streamfunction, temperature, salinity, density sections, and the vertically integrated heat transport. In addition the heatfunction shows whether the overturning circulation is transporting water at the correct temperature. Furthermore one could estimate the equivalent of the heatfunction for other tracers like salt, chemical and biological tracers providing additional tests on model skill.

The core of this paper was devoted to testing the impact of various physical processes on the ocean heat transport. A model of the ocean circulation was run where diapycnal mixing, high latitude convection, winds were selectively turned on and off. The heatfunction was used to

quantify the changes in heat transport. The main conclusions of the work are:

1) Abyssal mixing below 2000 m has a profound impact on the abyssal overturning circulation in the southern hemisphere, but it has hardly any effect on heat transport. Abyssal waters are formed through convection around Antarctica and return still cold to the surface south of the Antarctic Circumpolar Current, therefore never experiencing large temperature variations which is a requirement to transport large amounts of heat.

2) Strong mixing at the base of the thermocline acts to increase the ocean heat transport. For large diapycnal mixing rates ($\kappa \geq 0.3\times10^{-4}$ m^2 s^{-1}) the cold abyssal waters spreading from the Southern Ocean into the Pacific and Indian Oceans upwell into the subtropical thermoclines where they get warmed, resulting into a large heat transport. This result does not apply to the present climate, because mixing in the upper ocean is observed to be weak and there is no evidence of waters upwelling from the abyss into the subtropical thermoclines and contributing to ocean heat transport.

3) The deep waters formed through convection in the North Atlantic represent the northern limb of the overturning circulation that transports heat in the Atlantic Ocean. We compared the heat transport from two simulations in all identical except for the surface buoyancy fluxes in the North Atlantic. The simulation with present day forcing displayed vigorous convection at high latitudes and a peak heat transport of 0.8 PW in the North Atlantic. Convection was instead completely absent in the simulation with weaker buoyancy fluxes and resulted into a 0.3 PW of heat transport associated with the shallow wind-drive gyres. Hence water mass transformations at high latitudes contribute $\sim$60% of the North Atlantic heat transport and $\sim$40% of the total heat transport.

4) Winds are a crucial driver of ocean heat transport. The amount of heat transported by the oceans is linearly proportional to the magnitude of the wind stress (we did not study the dependence on the wind stress curl). In the Pacific and Indian Oceans this is obvious, because heat is transported by the shallow wind-driven gyre circulations in the tropics and subtropics. In the Atlantic Ocean, the additional heat transported by an overturning circulation that spans

the whole water column from low to high latitudes is also proportional to the wind stress – the strength of this circulation is sensitive to both local "local" northern hemisphere and "remote" southern hemisphere winds.

Two implications of these results are worth emphasizing. Abyssal mixing, defined as mixing below 2000 m, was shown to hardly affect the heat transport. Hence abyssal mixing by tides does not appear to be an important feedback for ocean heat transport. Similar conclusions have been reported from models that use more sophisticated parameterizations of abyssal mixing by tides (Saenko and Merryfield 2006).

A second interesting implication is that the heat transport associated with the deep circulations in the North Atlantic is as sensitive to winds as it is to high latitude convection. Numerous studies have shown that freshwater release by melting ice sheets can arrest North Atlantic Deep Water formation and the heat transport associated with the deep circulation in the Atlantic (e.g. Rahmstorf 1996). However these studies ignore the strong sensitivity of this circulation to changes in winds and atmospheric hydrological cycle, both expected to change if a massive ice sheet should melt. In Fig. 15 we show the vertically integrated heat transport from a simulation where we increased the winds by 50% and completely suppressed convection in the Northern Atlantic basin (a combination of the two experiments shown in Figs. 12 and 13). The result is compared to the control run forced with present day winds and freshwater fluxes (more details on the simulation are given in the figure caption). In the northern hemisphere the changes in heat transport are quite small because the decrease in ocean heat transport associated with the shut off of convection is largely compensated by the increase in wind-driven heat transport. The heat transport increases in the southern hemisphere where winds are the main driving mechanism. This simulation illustrates our point: any speculation on the role of high latitude convection on the ocean heat transport must consider the changes in wind patterns associated with the redistribution of ice masses and/or the ocean feedback on the atmospheric circulation. Furthermore it is changes in both low and high latitude winds that matters. The recent attention to the climate implications of shifts in winds over the Southern Ocean (Böning et al. 2008) must also be read with the realization that most of the

ocean heat transport is carried by the wind-driven gyres in the tropics and subtropics. FIG. 15

We did not discuss extensively the role of geostrophic eddies in driving ocean heat transport. We verified that the ocean heat transport is weakly sensitive to changes in the eddy diffusivity, the parameter that represents the strength of eddy mixing in the Gent and McWilliams (1990) parameterization used in our model. There are however reasons to suspect that this parameterization underestimates the role of eddies in driving ocean heat transport. First, the parameterization ignores variations in eddy diffusivity in response to changes in winds (Hallberg and Gnanadesikan 2006). Second, the parameterization does not include the diapycnal transport driven by eddies in the surface mixed layer (Marshall and Radko 2003; Greatbatch and Zhai 2007). We intend to pursue these issues in future studies.

Appendix A: Mass streamfunction in the presences of evaporation and precipitation

In this appendix we introduce the tracer transport function for a generic tracer satisfying the equation,

$$\frac{Dc}{Dt} = \mathcal{C}, \tag{17}$$

where $\mathcal{C}$ includes all processes that irreversibly modify the tracer concentration, i.e. mixing, source and sinks for chemical tracers, interaction with other species for biological tracers. Furthermore we will assume that there is a mass flux at the ocean surface, i.e. we allow for evaporation and precipitation: $E - P$.

Let us define the area $A(y, c, t)$ of that section below a certain value of tracer concentration c,

$$A(y, c, t) = \iint_{c' \leq c} \mathrm{d}x\mathrm{d}z. \tag{18}$$

The evolution equation for the area $A(y, c, t)$ is given by,

$$\frac{\partial A}{\partial t} = -\frac{\partial}{\partial y}\iint_{c' \leq c} v \ \mathrm{d}x\mathrm{d}z - \frac{\partial}{\partial c}\iint_{c' \leq c} \mathcal{C} \ \mathrm{d}x\mathrm{d}z - \int (E - P)\mathcal{H}(c - c_{surf}) \ \mathrm{d}x. \tag{19}$$

The last term is the increase/decrease in area $A(y, c, t)$ resulting from evaporation and precipitation of water with a value of tracer concentration $c = c_{surf}$. The function $\mathcal{H}$ is the Heaviside function which is equal to one for $c \geq c_{surf}$ and zero otherwise. The equation for $A(y, c, t)$ can be equivalently written as,

$$\frac{\partial A}{\partial t} = -\frac{\partial}{\partial y}\iint_{c' \leq c} v \ \mathrm{d}x\mathrm{d}z - \frac{\partial}{\partial c}\left[\iint_{c' \leq c} \mathcal{C} \ \mathrm{d}x\mathrm{d}z - \int (E - P)\,(c - c_{surf})\,\mathcal{H}(c - c_{surf}) \ \mathrm{d}x\right]. \tag{20}$$

Notice that in order to obtain this equation we used the fact that the Dirac delta function term resulting from the functional derivative of the Heaviside function vanishes because $(c - c_{surf})\,\delta(c - c_{surf}) = 0$.

A streamfunction and tracer transport function can now be defined in analogy to what done for heat in Eqs. (6) and (8),

$$\Psi(y, c) = \overline{\iint_{c' \leq c} v \ \mathrm{d}x\mathrm{d}z}, \qquad H(y, c) = \overline{\iint_{c' \leq c} \Psi(y, c) \ \mathrm{d}x\mathrm{d}z}. \tag{21}$$

The main implication of the surface mass flux is that the overturning streamfunction $\Psi(y, c)$ does not necessarily vanish at the ocean surface.

Appendix B: Calculation of the mass streamfunction in temperature coordinates

The overturning circulation in temperature coordinates, $\Psi(y, \theta)$, is computed as follows. The temperature and velocity fields, θ and v, are interpolated on a finer regular grid with a resolution of Δz = 10 m in order to have a good resolution in temperature space. The water column is then partitioned into a set of θ-layers, with a resolution of $\Delta\theta$= 1°K, and the meridional mass transport ($v + v_{GM}$) below each θ-level is computed. Finer and coarser resolutions were tested and found to produce very similar results. Summing the contributions to mass transport along each latitude, for each monthly mean and averaging over one year yields the result shown in Fig. 3c.

It is important that the interpolation on the finer z-grid conserves the mass and heat transport produced by the model. Since the model formulation predicts a transport within each z-layer, the same vertical structure was kept when interpolating onto a finer z-grid, yielding a staircaselike profile, as in the raw model outputs. This procedure exactly preserves the vertically integrated meridional mass transport at each grid point, but only approximately conserves the vertically integrated advective heat transport at each grid point. The error in the latter was found to never exceed 1%.

REFERENCES

Adcroft, A., C. Hill, and J. Marshall: 1997, Representation of topography by shaved cells in a height coordinate ocean model. *Monthly Weather Review*, **125**, 2293–2315.

Andrews, D. G.: 1983, A finite-amplitude eliassenpalm theorem in isentropic coordinates. *Journal of the Atmospheric Sciences*, **40**, 1877–1883.

Boccaletti, G., R. Ferrari, A. Adcroft, D. Ferreira, and J. C. Marshall: 2005, The vertical structure of ocean heat transport. *Geophysical Research Letters*, **32**, L10603, 1–4.

Böning, C. W., A. Dispert, M. Visbeck, S. R. Rintoul, and F. U. Schwarzkopf: 2008, The response of the antarctic circumpolar current to recent climate change. *Nature Geoscience*, **1**, 864–869.

Broeker, W. S.: 1991, The great ocean conveyor. *Oceanography*, **4**, 79–89.

Bryan, F.: 1986, High-latitude salinity effects and interhemispheric thermohaline circulations. *Science*, **323**, 301–304.

Bryan, F. and J. Sarmiento: 1985, Modeling ocean circulation. *Advances in Geophysics*, **28**, 433–459.

Bryan, K. and L. J. Lewis: 1979, A water mass model of the world ocean. *Journal of Geophysical Research*, **84**, 2503–2517.

Bryden, H. L. and S. Imawaki: 2001, Ocean heat transport. *Ocean Circulation and Climate*, 495–474.

Czaja, A. and J. Marshall: 2006, The partitioning of poleward heat transport between the atmosphere and ocean. *Journal of the Atmospheric Sciences*, **63**, 1498–1511.

Ferreira, D. and J. C. Marshall: 2006, Formulation and implementation of a residual-mean ocean circulation model. *Ocean Modeling*, **13**, 86–107.

Ganachaud, A. and C. Wunsch: 2003, Large-scale ocean heat and freshwater transports during the World Ocean Circulation Experiment. *Journal of Climate*, **16**, 696–705.

Garabato, A. C. N., K. L. Polzin, B. A. King, K. J. Heywood, and M. Visbeck: 2004, Widespread Intense Turbulent Mixing in the Southern Ocean. *Science*, **303**, 210–213.

Gent, P. R. and J. C. McWilliams: 1990, Isopycnal mixing in ocean circulation models. *Journal of Physical Oceanography*, **20**, 150–155.

Gerdes, R., C. Köberle, and J. Willebrand: 1991, The influence of numerical advection schemes on the results of ocean general circulation models. *Climate Dynamics*, **5**, 211–226.

Greatbatch, R. J. and X. Zhai: 2007, The generalized heat function. *Geophysical Research Letters*, **34**, L21601.

Hall, M. M. and H. L. Bryden: 1982, Direct estimates and mechanisms of ocean heat transport. *Deep-Sea Research*, **29**, 339–359.

Hallberg, R. and A. Gnanadesikan: 2006, The role of eddies in determining the structure and response of the wind-driven southern hemisphere overturning: Results from the modeling eddies in the southern ocean (meso) project. *Journal of Physical Oceanography*, **36**, 2232–2252.

Held, I. M.: 2001, The partitioning of the poleward energy transport between the tropical ocean and atmosphere. *Journal of the Atmospheric Sciences*, **58**, 943–948.

Ito, T. and J. Marshall: 2008, Control of lower-limb overturning circulation in the southern ocean by diapycnal mixing and mesoscale eddy transfer. *Journal of Physical Oceanography*, **38**, 2832–2845.

Jayne, S. R., L. C. S. Laurent, and S. T. Gille: 2004, Connections between ocean bottom topography and earth's climate. *Oceanography*, **17**, 65–74.

Jia: 2003, Ocean heat transport and its relationship to ocean circulation in the cmip coupled models. *Climate Dynamics*, **20**, 153–174.

Jiang, S., P. H. Stone, and P. Malanotte-Rizzoli: 1999, An assessment of the geophysical fluid dynamics laboratory ocean model with coarse resolution: Annual-mean climatology. *Journal of Geophysical Research*, **104**, 25623–25645.

Karsten, R. and J. Marshall: 2002, Constructing the residual circulation of the ACC from observations. *Journal of Physical Oceanography*, **32**, 3315–3327.

Klinger, B. A. and J. Marotzke: 2000, Meridional heat transport by the subtropical cell. *Journal*

of Physical Oceanography, **30**, 696–705.

Kuhlbrodt, T., A. Griesel, M. Montoya, A. Levermann, M. Hofmann, and S. Rahmstorf: 2007, On the driving processes of the atlantic meridional overturning circulation. *Rev. Geophys.*, **438**, RG2001.

Ledwell, J. R., A. J. Watson, and C. S. Law: 1993, Evidence for slow mixing across the pycnocline from an open ocean tracer release experiment. *Nature*, **364**, 701–703.

Levitus, S., R. Burgett, and T. Boyer: 1994, World Ocean Atlas 1994. vol 3: Salinity; vol. 4: Temperature. NOAA Atlas NESDIS 3 and 4, NOAA, U.S. Dept. of Commerce, Washington, D.C.

Marshall, J., C. Hill, L. Perelman, and A. Adcroft: 1997a, Hydrostatic, quasi-hydrostatic, and nonhydrostatic ocean modeling. *Journal of Geophysical Research*, **1**, 5733–5752.

Marshall, J. and T. Radko: 2003, Residual mean solutions for the antarctic circumpolar current and its associated overturning circulation. *Journal of Physical Oceanography*, **33**, 2341–2354.

Marshall, J. and F. Schott: 1999, Open ocean deep convection observations, models and theory. *Review of Geophysics*, **37**, 1–64.

Marshall, J. C., A. Adcroft, C. Hill, L. Perelman, and C. Heisey: 1997b, A finite-volume, incompressible navier stokes model for studies of the ocean on parallel computers. *Journal of Geophysical Research*, **102**, 5753–5766.

McDougall, T.: 2003, Potential enthalpy: A conservative oceanic variable for evaluating heat content and heat fluxes. *Journal of Physical Oceanography*, **33**, 945–963.

McDougall, T. and P. C. McIntosh: 2001, The temporal-residual mean velocity. part ii: Isopycnal interpretation and the tracer and momentum equations. *Journal of Physical Oceanography*, **31**, 1222–1246.

Munk, W. and L. Armi: 2001, Spirals on the sea: A manifestation of upper-ocean stirring. *Proceedings of the 12th 'Aha Huliko'a Hawaiian Winter Workshop*, 81–86.

Nurser, A. J. G. and M.-M. Lee: 2006, Isopycnal averaging at constant height. part i: The formulation and a case study. *Journal of Physical Oceanography*, **34**, 2721–2739.

Plumb, R. A. and R. Ferrari: 2005, Transformed eulerian-mean theory. i: Non-quasigeostrophic theory for eddies on a zonal mean flow. *Journal of Physical Oceanography*, **35**, 165–174.

Polzin, K. L., J. M. Toole, J. R. Ledwell, and R. W. Schmitt: 1997, Spatial Variability of Turbulent Mixing in the Abyssal Ocean. *Science*, **276**, 93–96.

Quadfasel, D.: 2005, The atlantic heat conveyor slows. *Nature*, **438**, 565–566.

Rahmstorf, S.: 1996, On the freshwater forcing and transport of the atlantic thermohaline circulation. *Climate Dyn.*, **12**, 799–811.

— 2002, Ocean circulation and climate during the past 120,000 years. *Nature*, **419**, 207–214.

Redi, M. H.: 1982, Oceanic isopycnal mixing by coordinate rotation. *Journal of Physical Oceanography*, **12**, 1154–1158.

Roemmich, D. and C. Wunsch: 1985, Two transatlantic sections: meridional circulation and heat flux in the subtropical north atlantic ocean. *Journal of Physical Oceanography*, **32**, 619–664.

Saenko, O. A. and W. J. Merryfield: 2005, On the effect of topographically-enhanced mixing on the global ocean circulation. *Journal of Physical Oceanography*, **35**, 826–834.

— 2006, Vertical partition of ocean heat transport in isothermal coordinates. *Geophysical Research Letters*, **33**, L01606.

Saenko, O. A. and A. J. Weaver: 2004, What drives heat transport in the atlantic: Sensitivity to mechanical energy supply and buoyancy forcing in the southern ocean. *Geophysical Research Letters*, **31**, 281–314.

Scott, J. R. and J. Marotzke: 2002, The location of diapycnal mixing and the meridional overturning circulation. *Journal of Physical Oceanography*, **32**, 3578–3593.

Simmons, H. L., S. R. Jayne, L. C. S. Laurent, and A. J. Weaver: 2004, Tidally driven mixing in a numerical model of the ocean general circulation. *Ocean Modelling*, **6**, 245–263.

Talley, L.: 2003, Shallow, intermediate and deep overturning components of the global heat budget. *Journal of Physical Oceanography*, **33**, 530–560.

Toggweiller, J. R. and B. Samuels: 1995, Effect of drake passage on the global thermohaline circulation. *Deep-Sea Research*, **42**, 477–500.

Trenberth, W. G. L., K. E. and J. G. Olson: 1990, The mean annual cycle in global ocean wind stress. *Journal of Physical Oceanography*, **20**, 1742–1760.

Vallis, G. K.: 2000, Large-scale circulation and production of stratification: effects of wind, geometry and diffusion. *Journal of Physical Oceanography*, **30**, 933–954.

— 2006, *Atmospheric and Oceanic Fluid Dynamics: Fundamentals and Large-scale Circulation*. Cambridge University Press, Cambridge, 1st edition, 745 + xxv pp.

Vallis, G. K. and R. Farneti: 2009, Meridional energy transport in the coupled atmosphere-ocean system: scaling and numerical experiments. *Quarterly Journal of the Royal Meteorological Society*, **135**, 1699–1720.

Wofe, C. L. and P. Cessi: 2010, What sets the strength of the middepth stratification and overturning circulation in eddying ocean models? *Journal of Physical Oceanography*, **40**, 1520–1538.

Wunsch, C.: 2010, Towards understanding the paleocean. *Quat. Science Rev.*, **29**, 1960–1967.

Wunsch, C. and R. Ferrari: 2004, Vertical mixing, energy, and the general circulation of the ocean. *Ann. Rev. Fluid Mech.*, **36**, 281–314.

Figure Captions

FIG. 1. The three panels represent an idealized overturning circulation as a function of latitude and temperature. The bell shaped upper edge of the domain represents the ocean surface temperature decreasing from the equator to the poles. Each panel sketches the balance between the northward OHT across a fixed latitude and diabatic heating to the north. (a) The OHT across a latitude and below a certain temperature θ is balanced by diabatic heating between the latitude considered and the northern edge of the ocean. The heatfunction $H(y, \theta)$ represents this OHT. (b) The OHT associated with a closed circulation is given by the diabatic heating in the area between the latitude considered and the latitude reached to the north by that circulation. The relationship between this OHT and the heatfunction is given in Eq. (9). (c) The meridional OHT associated with a circulation embedded in another flow is also given by the diabatic heating in the area between the latitude considered and the latitude reached to the north by that circulation.

FIG. 2. The three panels represent three possible overturning circulations for idealized oceans. In the first panel there are only two isolated overturning cells at warm temperatures. In the second panel there is a single deep overturning cell at cold temperatures. In the third panel, given by the sum of the circulations in the first two, the surface and deep cells are connected. The shaded area represent the area of diabatic heating that balances the meridional OHT across 20°N for each circulation.

FIG. 3. Three versions of the overturning streamfunction (in Sv) for the control simulation. (left) The streamfunction associated with the zonally integrated Eulerian velocity as defined in Eq. (12). (middle) The streamfunction associated with the sum of the zonally integrated Eulerian and eddy-induced velocities, see Eq. (13). (right) The streamfunction associated with the zonal integral at fixed temperature of the sum of the Eulerian and eddy-induced velocities, see Eq. (14). The contour interval is 5 Sv. Clockwise and counter-clockwise circulations are denoted by solid and dashed lines, respectively. The zero contour is highlighted.

FIG. 4. Ocean heat transport (in PW, with positive values representing northward transport) for the control run (solid line) and from analysis of individual hydrographic sections at a few latitudes (crosses) as described in Ganachaud and Wunsch (2003). The dashed line represents the mean heat flux imposed at the ocean surface in all the model runs (e.g. Jiang et al. 1999). The difference between the simulated ocean heat transport (solid) and the imposed surface heat flux (dashed) is due to the restoring term.

FIG. 5. (a) Streamfunction in latitude-temperature space for the control run. (b) The corresponding heatfunction, whose contours describe the pathways of heat, vanishes where no heat is being transported by the ocean circulation. It is positive (negative) for heat moving northward (southward). The topmost value of the heatfunction equals the total advective heat transport. In the top and middle panels, black dashed lines represent the yearly mean and minimum surface temperature (based on monthly averaged data) at each latitude. (c) Total advective heat transport (solid black) and its partitioning among the four closed circulations visible in the top panel: the contribution of the two shallow warm cells (dashed black) and the two deep cold cells associated with

AABW and NADW (solid grey). The grey dashed line is the residual heat transport that cannot be ascribed to individual circulations and is carried by a combination of the north hemisphere warm cell and the NADW cell, here referred to as the *mixed* circulation.

FIG. 6. (a) Streamfunction in latitude-temperature space, (b) heatfunction and (c) decomposition of the OHT among the various circulations for the Atlantic Ocean in the control run. Notations are as in Fig. 5.

FIG. 7. (a) Streamfunction in latitude-temperature space, (b) heatfunction and (c) decomposition of the OHT among the various circulations for the Indo-Pacific Ocean in the control run. Notations are as in Fig. 5.

FIG. 8. (a) Streamfunction in latitude-temperature space, (b) heatfunction and (c) decomposition of the OHT among the various circulations for the global ocean in the enhanced abyssal mixing run (κ is set to 0.3×10^{-4} m^2 s^{-1} above 2000 m and to 1.7×10^{-4} m^2 s^{-1} below). Notations are as in Fig. 5.

FIG. 9. (a) Streamfunction in latitude-temperature space, (b) heatfunction and (c) decomposition of the OHT among the various circulations for the global ocean in the run with enhanced uniform mixing (κ is 1×10^{-4} m^2 s $^{-1}$ everywhere, i.e. three times the value used in the control run). Notations are as in Fig. 5.

FIG. 10. (a) Streamfunction in latitude-temperature space, (b) heatfunction and (c) decomposition of the OHT among the various circulations for the Pacific Ocean in the run with enhanced uniform

mixing (κ is 1×10^{-4} m^2 s^{-1} everywhere, i.e. three times the value used in the control run). Notations are as in Fig. 5.

FIG. 11. Maximum value of the heatfunction in the southern hemisphere for the warm (solid), cold (dot-dashed), and mixed (dashed) circulations from four different simulations run with uniform diffusivities of κ=(0.2,0.3,0.5,1.0)$\times10^{-4}$ m^2 s.

FIG. 12. (a) Streamfunction in latitude-temperature space, (b) heatfunction and (c) decomposition of the OHT among the various circulations for the Atlantic Ocean in the "water-hosing" run (i.e., a simulation where the value of the surface salinity restoring north of 50°N has been decreased by 2 psu). Note that the deep overturning cell associated with NADW has disappeared. Notations are as in Fig. 5.

FIG. 13. (a) Streamfunction in latitude-temperature space, (b) heatfunction and (c) decomposition of the OHT among the various circulations for the global ocean in a run with twice the wind stress used in the control run. Notations are as in Fig. 5.

FIG. 14. (left) Maximum value of the warm and cold overturning cells in the northern hemisphere and their separatrix streamline Ψ_{mixed} from four different simulations where the wind stress was 0.5, 1.0, 1.5 and 2 times the value used in the control run. (right) Corresponding maximum value of the heatfunction for each overturning cell.

FIG. 15. Total OHT as a function of latitude from two different simulations: the control run shown in Fig. 4 (solid) and a simulation in all equal to the control run except that the value of the surface

salinity restoring north of 50°N in the North Atlantic has been decreased by 2 psu and the global wind stress has been multiplied by a factor of 1.5 (dashed).

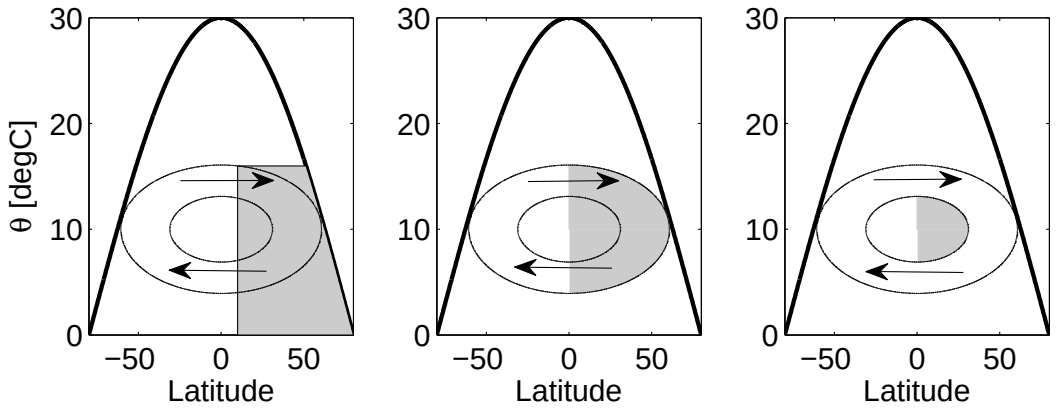

FIG. 1. The three panels represent an idealized overturning circulation as a function of latitude and temperature. The bell shaped upper edge of the domain represents the ocean surface temperature decreasing from the equator to the poles. Each panel sketches the balance between the northward OHT across a fixed latitude and diabatic heating to the north. (a) The OHT across a latitude and below a certain temperature θ is balanced by diabatic heating between the latitude considered and the northern edge of the ocean. The heatfunction $H(y, \theta)$ represents this OHT. (b) The OHT associated with a closed circulation is given by the diabatic heating in the area between the latitude considered and the latitude reached to the north by that circulation. The relationship between this OHT and the heatfunction is given in Eq. (9). (c) The meridional OHT associated with a circulation embedded in another flow is also given by the diabatic heating in the area between the latitude considered and the latitude reached to the north by that circulation.

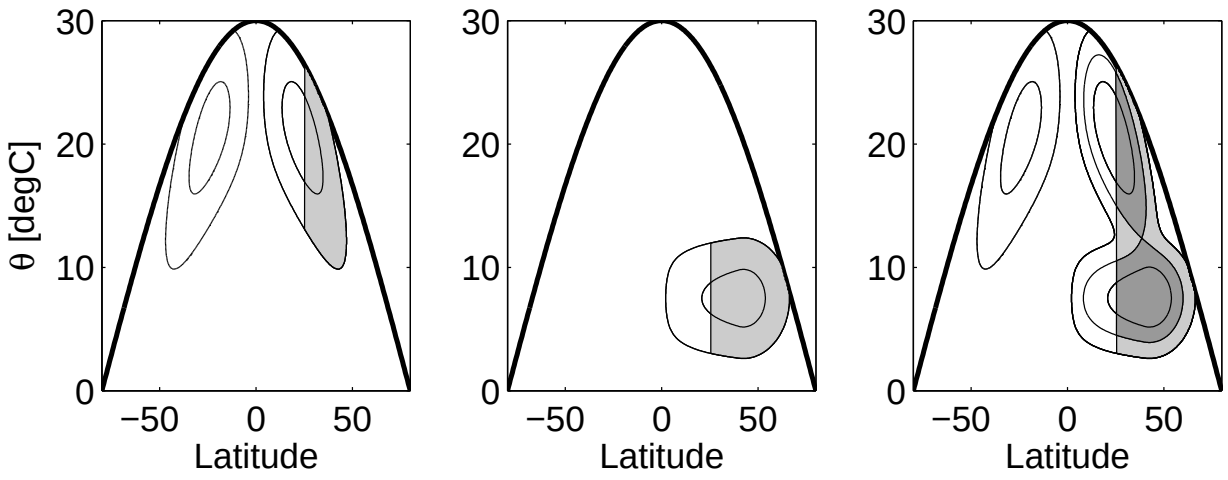

FIG. 2. The three panels represent three possible overturning circulations for idealized oceans. In the first panel there are only two isolated overturning cells at warm temperatures. In the second panel there is a single deep overturning cell at cold temperatures. In the third panel, given by the sum of the circulations in the first two, the surface and deep cells are connected. The shaded area represent the area of diabatic heating that balances the meridional OHT across 20°N for each circulation.

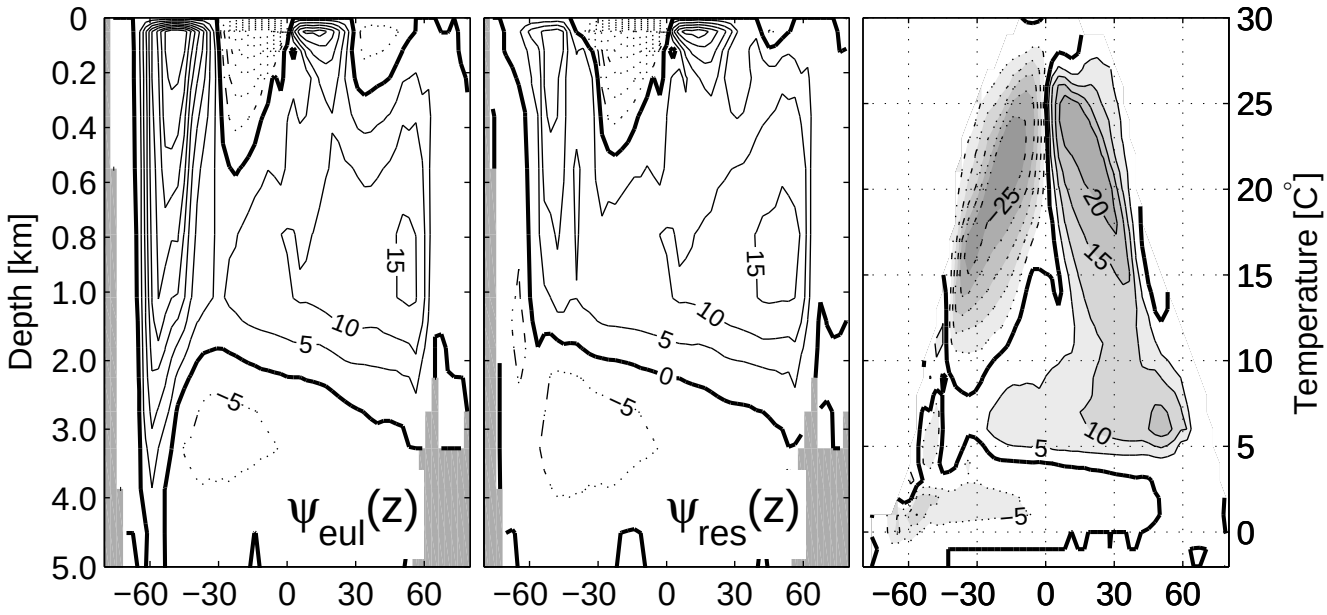

FIG. 3. Three versions of the overturning streamfunction (in Sv) for the control simulation. (left) The streamfunction associated with the zonally integrated Eulerian velocity as defined in Eq. (12). (middle) The streamfunction associated with the sum of the zonally integrated Eulerian and eddy-induced velocities, see Eq. (13). (right) The streamfunction associated with the zonal integral at fixed temperature of the sum of the Eulerian and eddy-induced velocities, see Eq. (14). The contour interval is 5 Sv. Clockwise and counter-clockwise circulations are denoted by solid and dashed lines, respectively. The zero contour is highlighted.

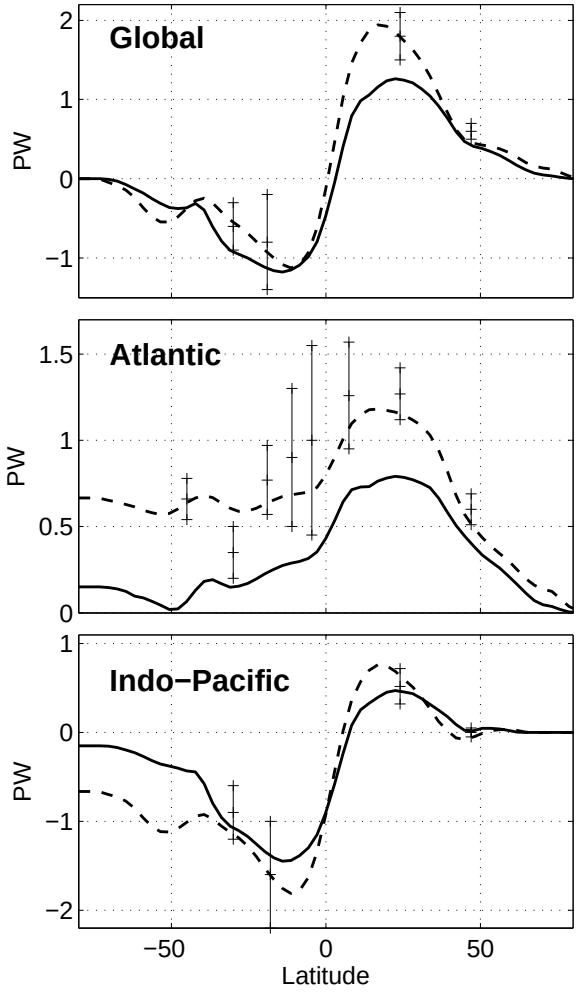

FIG. 4. Ocean heat transport (in PW, with positive values representing northward transport) for the control run (solid line) and from analysis of individual hydrographic sections at a few latitudes (crosses) as described in Ganachaud and Wunsch (2003). The dashed line represents the mean heat flux imposed at the ocean surface in all the model runs (e.g. Jiang et al. 1999). The difference between the simulated ocean heat transport (solid) and the imposed surface heat flux (dashed) is due to the restoring term.

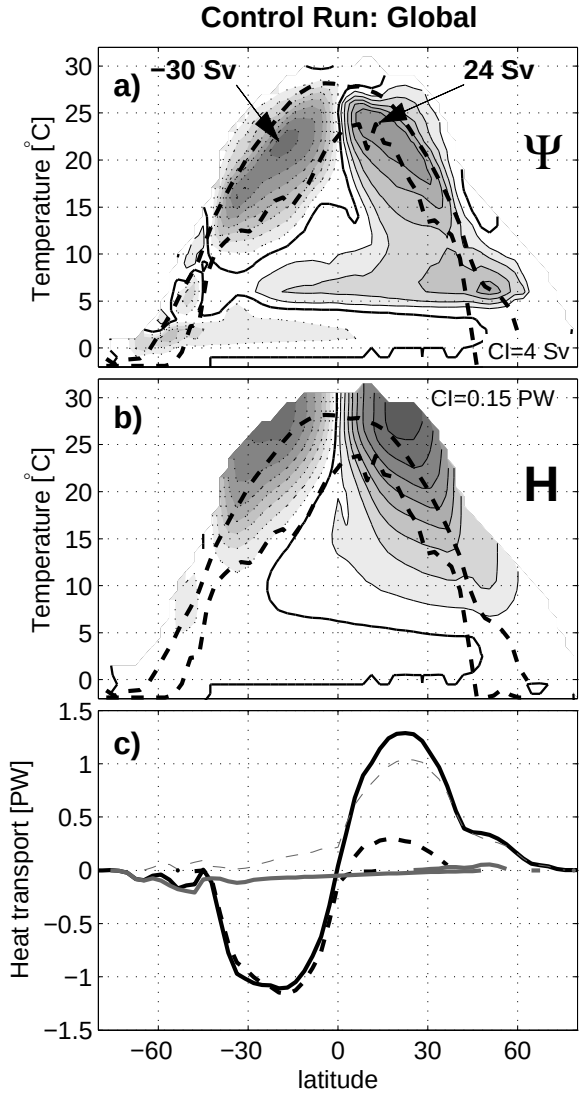

FIG. 5. (a) Streamfunction in latitude-temperature space for the control run. (b) The corresponding heatfunction, whose contours describe the pathways of heat, vanishes where no heat is being transported by the ocean circulation. It is positive (negative) for heat moving northward (southward). The topmost value of the heatfunction equals the total advective heat transport. In the top and middle panels, black dashed lines represent the yearly mean and minimum surface temperature (based on monthly averaged data) at each latitude. (c) Total advective heat transport (solid black) and its partitioning among the four closed circulations visible in the top panel: the contribution of the two shallow warm cells (dashed black) and the two deep cold cells associated with AABW and NADW (solid grey). The grey dashed line is the residual heat transport that cannot be ascribed to individual circulations and is carried by a combination of the north hemisphere warm cell and the NADW cell, here referred to as the *mixed* circulation.

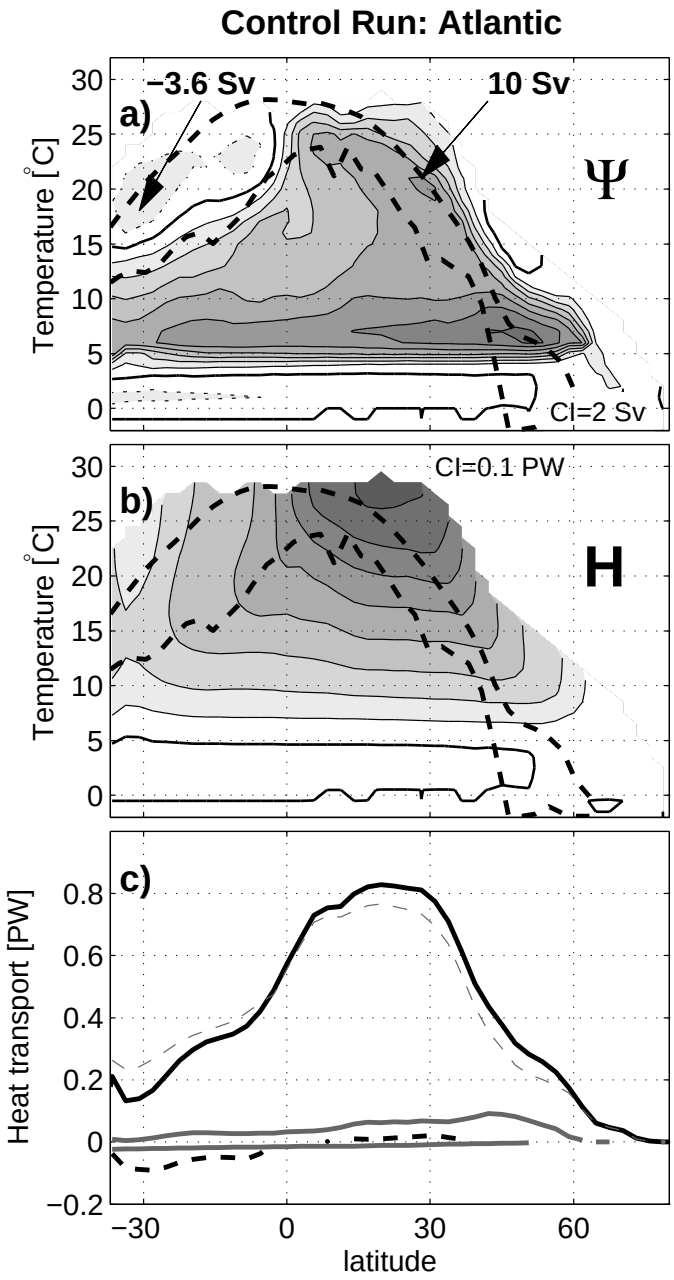

FIG. 6. (a) Streamfunction in latitude-temperature space, (b) heatfunction and (c) decomposition of the OHT among the various circulations for the Atlantic Ocean in the control run. Notations are as in Fig. 5.

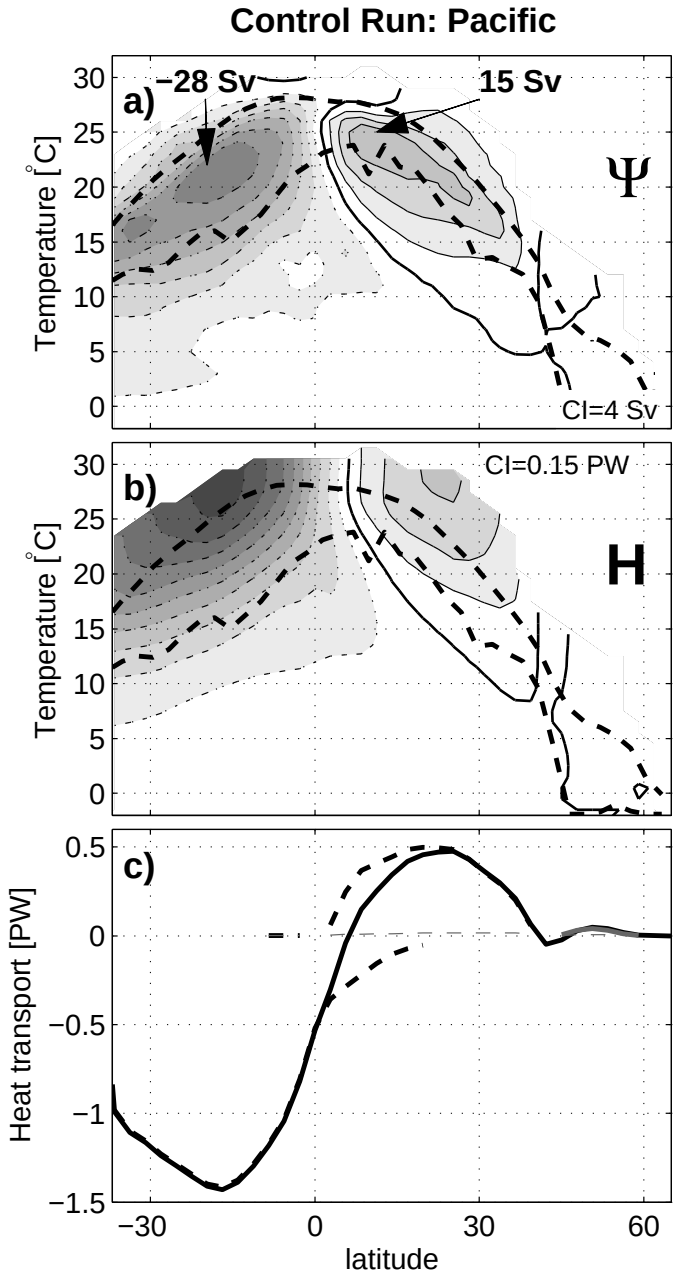

FIG. 7. (a) Streamfunction in latitude-temperature space, (b) heatfunction and (c) decomposition of the OHT among the various circulations for the Indo-Pacific Ocean in the control run. Notations are as in Fig. 5.

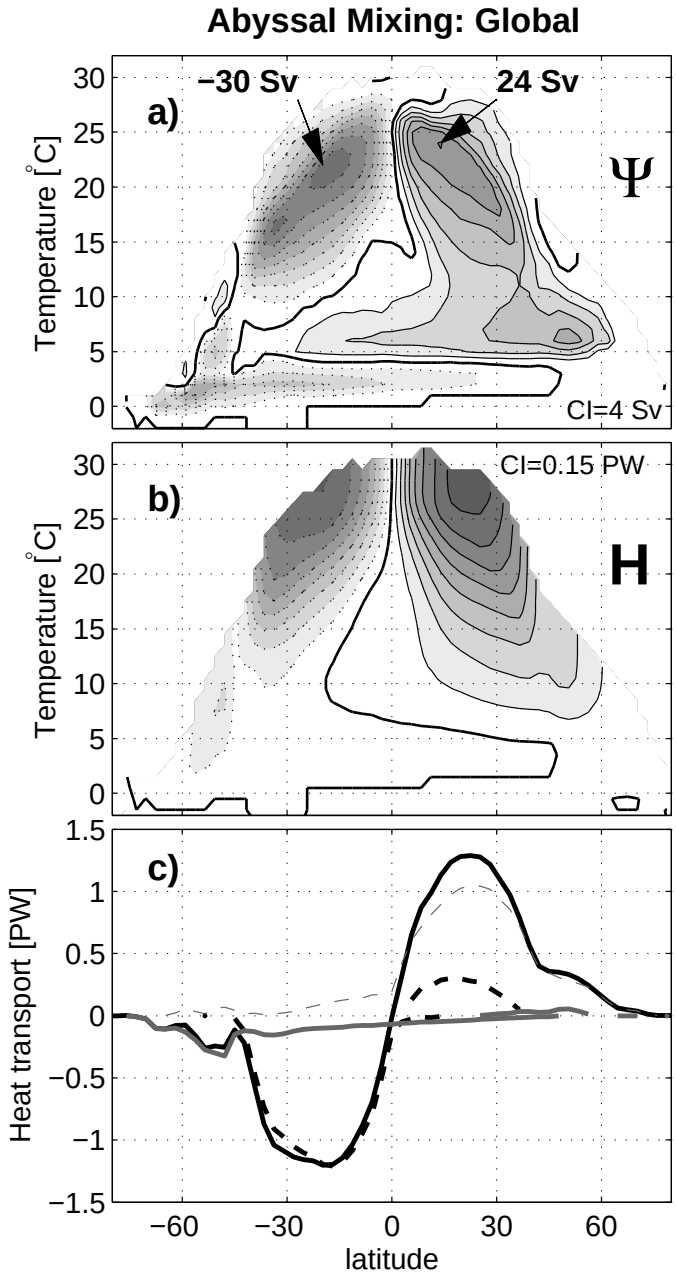

FIG. 8. (a) Streamfunction in latitude-temperature space, (b) heatfunction and (c) decomposition of the OHT among the various circulations for the global ocean in the enhanced abyssal mixing run (κ is set to 0.3×10^{-4} m^2 s^{-1} above 2000 m and to 1.7×10^{-4} m^2 s^{-1} below). Notations are as in Fig. 5.

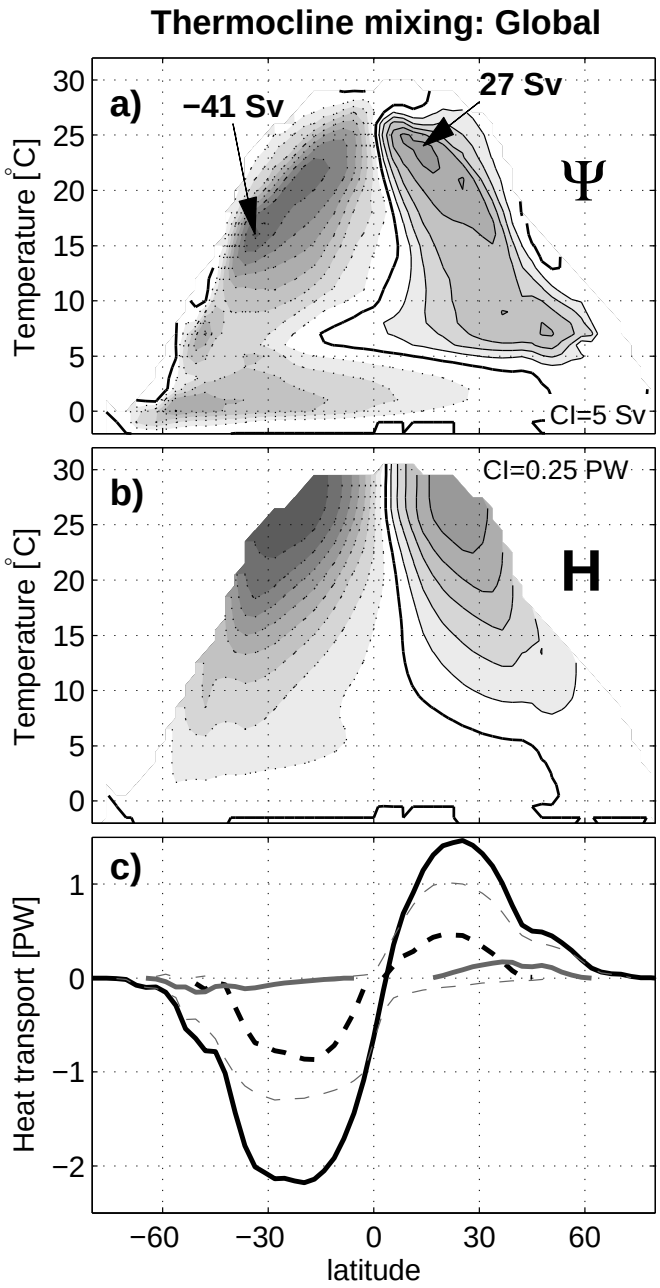

FIG. 9. (a) Streamfunction in latitude-temperature space, (b) heatfunction and (c) decomposition of the OHT among the various circulations for the global ocean in the run with enhanced uniform mixing (κ is 1×10^{-4} m^2 s^{-1} everywhere, i.e. three times the value used in the control run). Notations are as in Fig. 5.

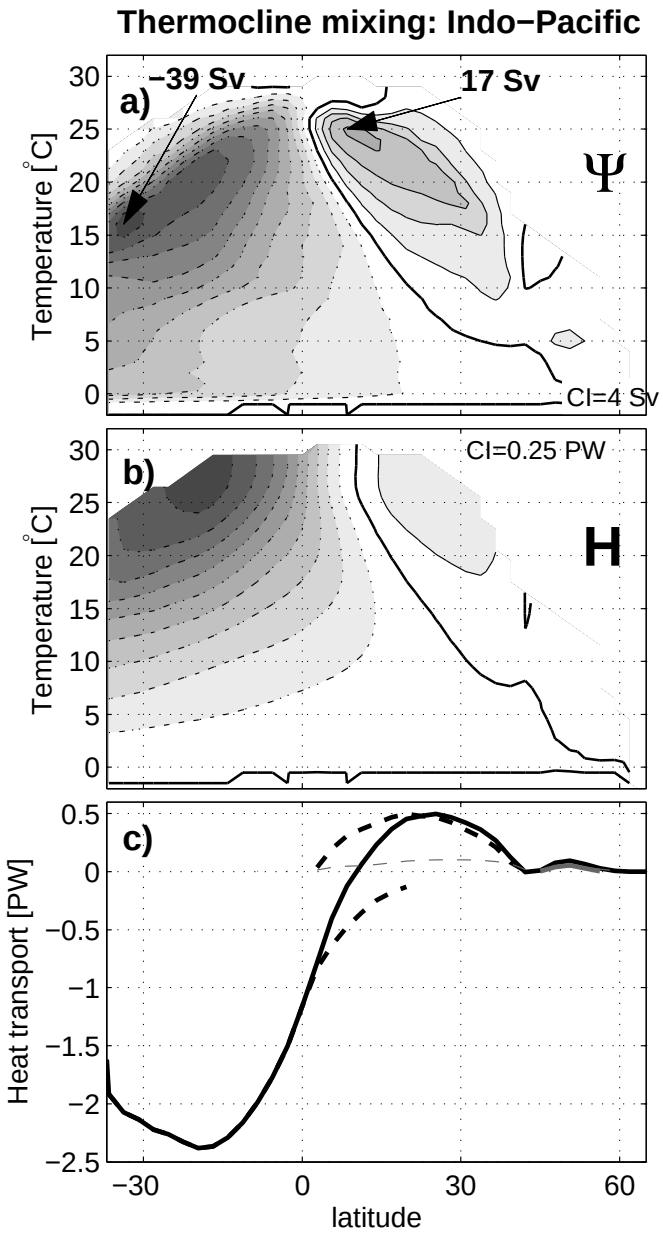

FIG. 10. (a) Streamfunction in latitude-temperature space, (b) heatfunction and (c) decomposition of the OHT among the various circulations for the Pacific Ocean in the run with enhanced uniform mixing (κ is 1×10^{-4} m^2 s^{-1} everywhere, i.e. three times the value used in the control run). Notations are as in Fig. 5.

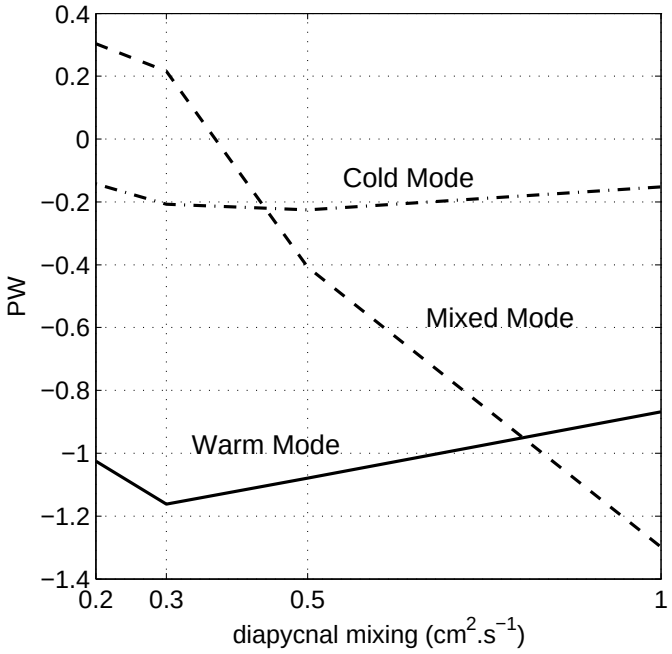

FIG. 11. Maximum value of the heatfunction in the southern hemisphere for the warm (solid), cold (dot-dashed), and mixed (dashed) circulations from four different simulations run with uniform diffusivities of κ=(0.2,0.3,0.5,1.0)$\times 10^{-4}$ m^2 s.

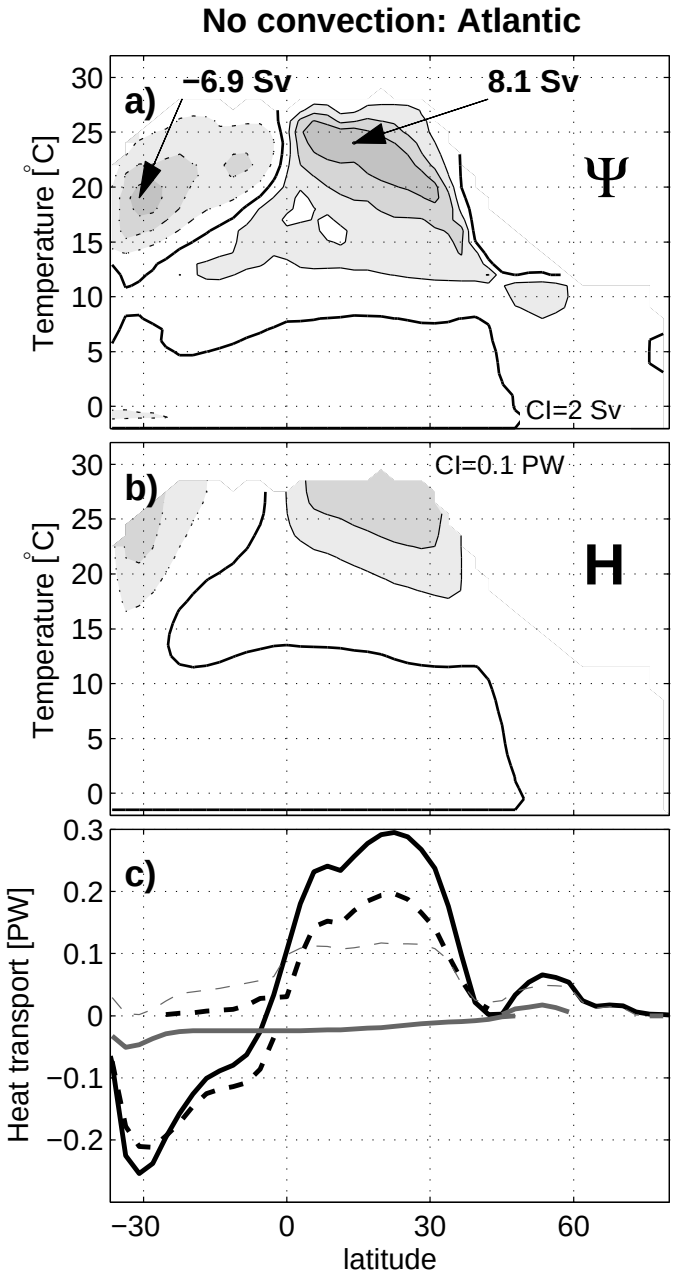

FIG. 12. (a) Streamfunction in latitude-temperature space, (b) heatfunction and (c) decomposition of the OHT among the various circulations for the Atlantic Ocean in the "water-hosing" run (i.e., a simulation where the value of the surface salinity restoring north of 50°N has been decreased by 2 psu). Note that the deep overturning cell associated with NADW has disappeared. Notations are as in Fig. 5.

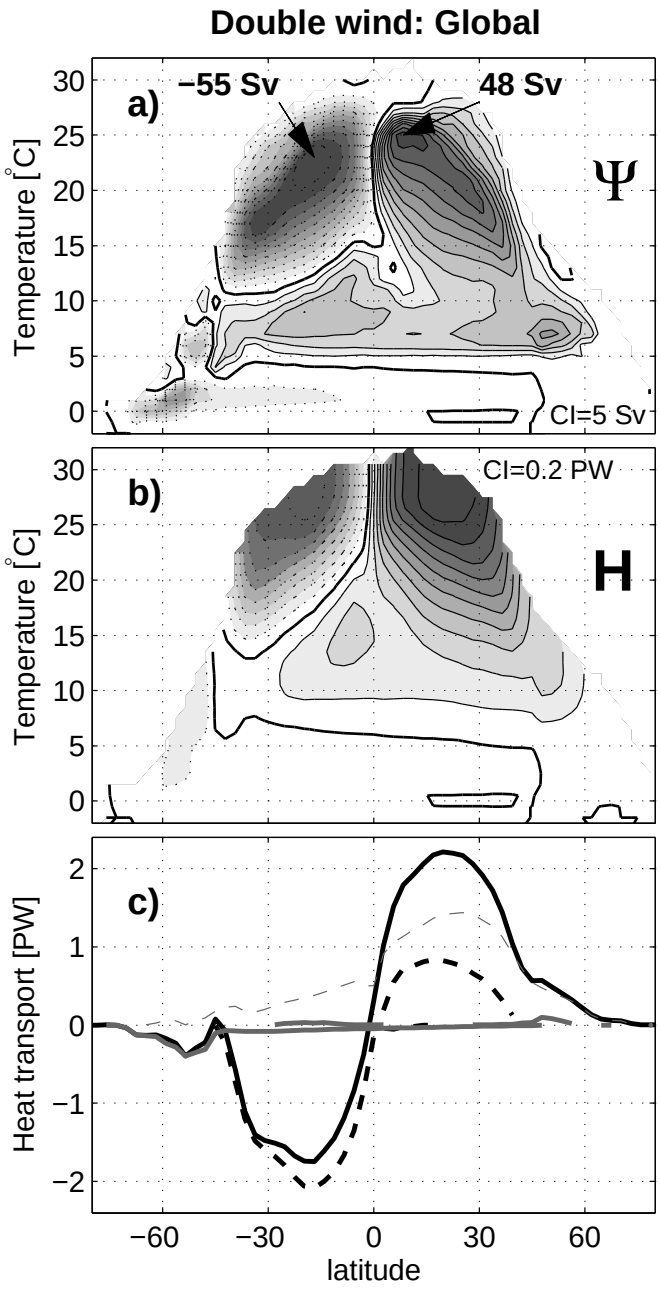

FIG. 13. (a) Streamfunction in latitude-temperature space, (b) heatfunction and (c) decomposition of the OHT among the various circulations for the global ocean in a run with twice the wind stress used in the control run. Notations are as in Fig. 5.

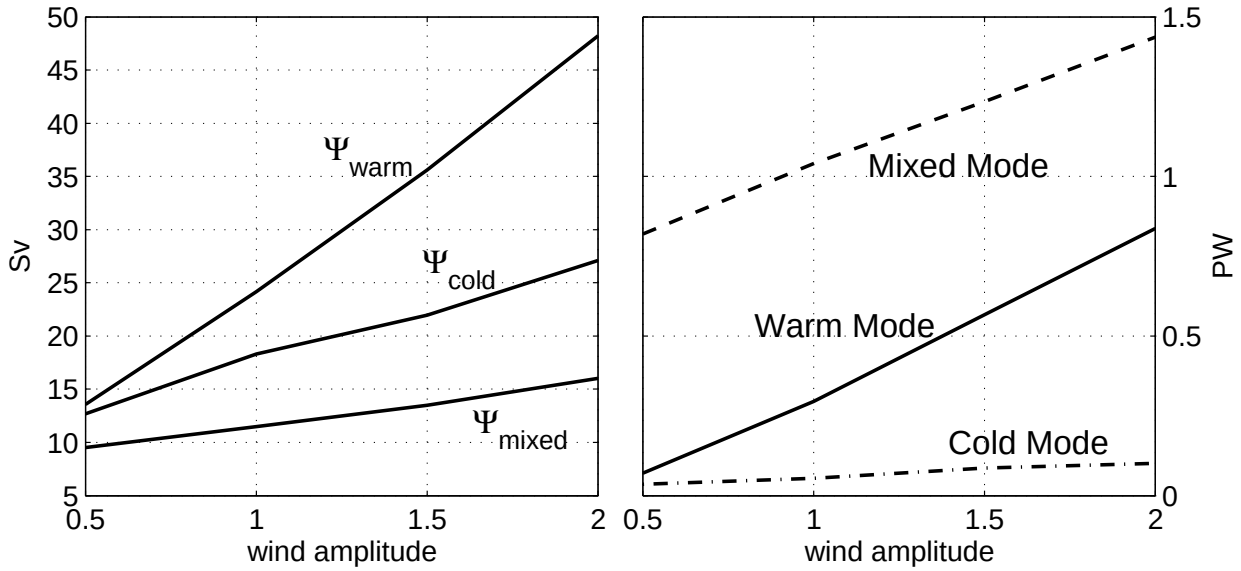

FIG. 14. (left) Maximum value of the warm and cold overturning cells in the northern hemisphere and their separatrix streamline Ψ_{mixed} from four different simulations where the wind stress was 0.5, 1.0, 1.5 and 2 times the value used in the control run. (right) Corresponding maximum value of the heatfunction for each overturning cell.

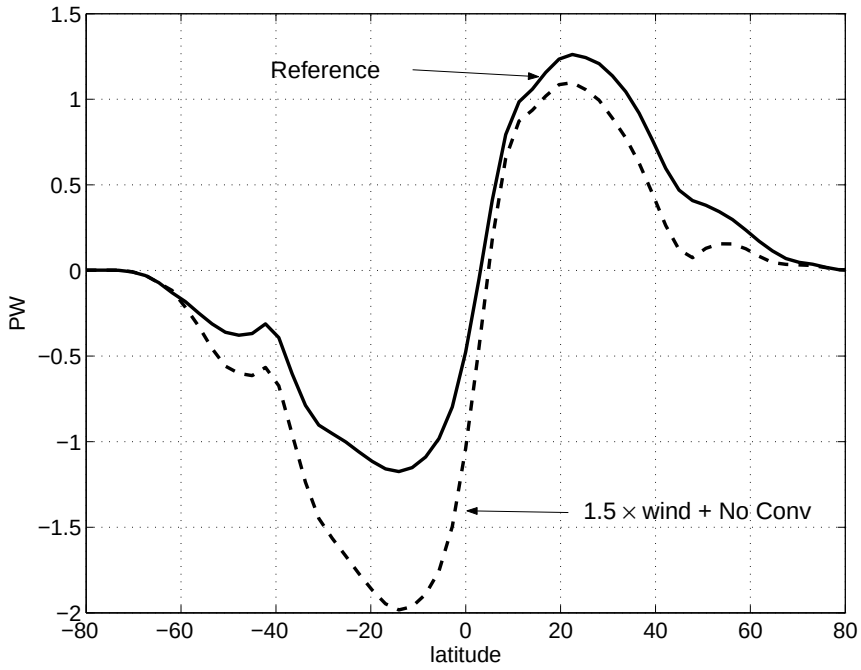

FIG. 15. Total OHT as a function of latitude from two different simulations: the control run shown in Fig. 4 (solid) and a simulation in all equal to the control run except that the value of the surface salinity restoring north of 50°N in the North Atlantic has been decreased by 2 psu and the global wind stress has been multiplied by a factor of 1.5 (dashed).